

# New Insight Into Mechanisms of Hepatic Encephalopathy: An Integrative Analysis Approach to Identify Molecular Markers and Therapeutic Targets

## 肝性脑病发病机制的新见解：一种识别分子标志物和治疗靶点的综合分析方法

Ali Sepehrinezhad<sup>1,2</sup>, Ali Shahbazi<sup>1,3</sup>, Sajad Sahab Negah<sup>2,4</sup> and Fin Stolze Larsen<sup>5</sup>

阿里·塞佩赫里内扎德<sup>1,2</sup>、阿里·沙赫巴齐<sup>1,3</sup>、萨贾德·萨哈布·内加<sup>2,4</sup>和芬·斯托尔泽·拉森<sup>5</sup>

<sup>1</sup> Department of Neuroscience, Faculty of Advanced Technologies in Medicine, Iran University of Medical Sciences, Tehran, Iran. <sup>2</sup> Neuroscience Research Center, Mashhad University of Medical Sciences, Mashhad, Iran. <sup>3</sup> Cellular and Molecular Research Center, Iran University of Medical Sciences, Tehran, Iran. <sup>4</sup> Department of Neuroscience, Faculty of Medicine, Mashhad University of Medical Sciences, Mashhad, Iran. <sup>5</sup> Department of Hepatology CA-3163, Rigshospitalet, Copenhagen University Hospital, Copenhagen, Denmark.

<sup>1</sup> 伊朗医科大学医学先进技术学院神经科学系，德黑兰，伊朗。<sup>2</sup> 马什哈德医科大学神经科学研究中心，马什哈德，伊朗。<sup>3</sup> 伊朗医科大学细胞与分子研究中心，德黑兰，伊朗。<sup>4</sup> 马什哈德医科大学医学院神经科学系，马什哈德，伊朗。<sup>5</sup> 丹麦哥本哈根大学医院里格医院肝病科 CA - 3163，哥本哈根，丹麦。

**ABSTRACT:** Hepatic encephalopathy (HE) is a set of complex neurological complications that arise from advanced liver disease. The precise molecular and cellular mechanism of HE is not fully understood. Differentially expressed genes (DEGs) from microarray technologies are powerful approaches to obtain new insight into the pathophysiology of HE. We analyzed microarray data sets of cirrhotic patients with HE from Gene Expression Omnibus to identify DEGs in postmortem cerebral tissues. Consequently, we uploaded significant DEGs into the STRING to specify protein-protein interactions. Cytoscape was used to reconstruct the genetic network and identify hub genes. Target genes were uploaded to different databases to perform comprehensive enrichment analysis and repurpose new therapeutic options for HE. A total of 457 DEGs were identified in 2 data sets totally from 12 cirrhotic patients with HE compared with 12 healthy subjects. We found that 274 genes were upregulated and 183 genes were downregulated. Network analyses on significant DEGs indicated 12 hub genes associated with HE. Enrichment analysis identified fatty acid beta-oxidation, cerebral organic acidurias, and regulation of actin cytoskeleton as main involved pathways associated with upregulated genes; serotonin receptor 2 and ELK-SRF/GATA4 signaling, GPCRs, class A rhodopsin-like, and p38 MAPK signaling pathway were related to downregulated genes. Finally, we predicted 39 probable effective drugs/agents for HE. This study not only confirms main important involved mechanisms of HE but also reveals some yet unknown activated molecular and cellular pathways in human HE. In addition, new targets were identified that could be of value in the future study of HE.

**摘要:** 肝性脑病 (HE) 是一组由晚期肝病引发的复杂神经并发症。HE 的确切分子和细胞机制尚未完全明确。利用微阵列技术分析差异表达基因 (DEGs) 是深入了解 HE 病理生理学的有力手段。我们分析了来自基因表达综合数据库 (Gene Expression Omnibus) 的 HE 肝硬化患者的微阵列数据集, 以确定死后脑组织中的 DEGs。随后, 我们将显著的 DEGs 上传至 STRING 数据库以明确蛋白质 - 蛋白质相互作用。使用 Cytoscape 软件重建基因网络并识别枢纽基因。将靶基因上传至不同数据库, 以对 HE 进行全面的富集分析并重新挖掘新的治疗方案。与 12 名健康受试者相比, 在来自 12 名 HE 肝硬化患者的 2 个数据集中共鉴定出 457 个 DEGs。我们发现 274 个基因表达上调, 183 个基因表达下调。对显著 DEGs 的网络分析表明, 有 12 个枢纽基因与 HE 相关。富集分析确定脂肪酸  $\beta$ -氧化、脑有机酸尿症和肌动蛋白细胞骨架调节是与上调基因相关的主要通路; 血清素受体 2 和 ELK - SRF/GATA4 信号通路、A 类视紫红质样 G 蛋白偶联受体 (GPCRs) 和 p38 丝裂原活化蛋白激酶 (MAPK) 信号通路与下调基因相关。最后, 我们预测了 39 种可能对 HE 有效的药物/制剂。本研究不仅证实了 HE 的主要重要发病机制, 还揭示了人类 HE 中一些尚未知晓的激活的分子和细胞通路。此外, 还确定了一些新的靶点, 这些靶点可能在未来 HE 的研究中具有重要价值。

**KEYWORDS:** Cirrhosis, hepatic encephalopathy, bioinformatics analysis, differentially expressed genes, drug repurposing

**关键词:** 肝硬化; 肝性脑病; 生物信息学分析; 差异表达基因; 药物再利用

**RECEIVED:** August 9, 2022. **ACCEPTED:** January 17, 2023.

**收稿日期:**2022 年 8 月 9 日。 **录用日期:**2023 年 1 月 17 日。

**TYPE:** Original Research Article

**文章类型:** 原创研究论文

**FUNDING:** The author(s) received no financial support for the research, authorship, and/or publication of this article.

**资助信息:** 作者在该研究、论文撰写和/或发表过程中未获得任何资金支持。

**DECLARATION OF CONFLICTING INTERESTS:** The author(s) declared no potential conflicts of interest with respect to the research, authorship, and/or publication of this article.

**利益冲突声明:** 作者声明在该研究、论文撰写和/或发表过程中不存在潜在利益冲突。

**CORRESPONDING AUTHORS:** Ali Shahbazi, Department of Neuroscience, Faculty of Advanced Technologies in Medicine, Iran University of Medical Sciences, Tehran, 1449614535, Iran. Email: shahbazi.a@iums.ac.ir

**通信作者:** 阿里·沙赫巴齐, 伊朗医科大学医学先进技术学院神经科学系, 德黑兰, 1449614535, 伊朗。邮箱:shahbazi.a@iums.ac.ir

Fin Stolze Larsen, Department of Hepatology CA-3163, Rigshospitalet, Copenhagen University Hospital, Copenhagen, Denmark. Email: Stolze@post3.tele.dk

## Introduction

### 引言

Hepatic encephalopathy (HE) develops in more than 60% of cirrhotic patients and is associated with a poor prognosis.<sup>1</sup> Hepatic encephalopathy following liver failure is a neuropsychiatric syndrome ranging from mild confusion, irritability, lethargy, disorientation, and sleep disturbances in the mildest forms to severe confusion, deep coma, positive Babinski sign, seizures, and cerebral edema.<sup>2</sup> Hepatic encephalopathy is the main cause of readmission to the hospital, has negative effects on quality of life, increases health care costs, and is directly related to a high mortality rate with a survival rate of 36% at 1 year.<sup>3</sup> Patients with a previous history of HE have a 40% risk of recurring HE during 1 year.<sup>4</sup> Neuroinflammation, blood-brain barrier (BBB) permeabilization, astrocyte swelling, intracranial hypertension, and cerebral herniation are main pathological cerebral findings in more fulminant cases.<sup>5,6</sup> The precise cellular and molecular mechanism of HE is, however still poorly understood. The current view is that cerebral accumulation of ammonia, glutamine, and gut-derived neurotoxic agents such as mercaptans, cytokines, lipopolysaccharide, and benzodiazepine-like substances activate microglia cells and trigger some important inflammatory downstream signaling, induce astrocyte dysfunction, disturb brain homeostasis, neuro-degeneration, and consequently onset of HE.<sup>7</sup> Pharmacological prescription for treatment of HE is often effective, but liver transplantation is the only curative therapeutic procedure for HE in patients with end-stage liver disease.<sup>8</sup> We here performed an integrative bioinformatic study on transcriptomic data from cerebral tissues in cirrhotic patients with HE to identify all the mechanisms of liver coma through multiplatform-enriched biological signatures, brain region explorations, and posttranscriptional targeting.

肝性脑病 (HE) 在超过 60% 的肝硬化患者中发生, 并且与预后不良相关。<sup>1</sup> 肝衰竭后的肝性脑病是一种神经精神综合征, 其表现从轻到重, 轻者表现为轻度意识模糊、易怒、嗜睡、定向障碍和睡眠障碍, 重者表现为严重意识模糊、深度昏迷、巴宾斯基征阳性、癫痫发作和脑水肿。<sup>2</sup> 肝性脑病是患者再次入院的主要原因, 对生活质量产生负面影响, 增加医疗成本, 并且与高死亡率直接相关, 1 年生存率为 36%。<sup>3</sup> 有肝性脑病既往史的患者在 1 年内有 40% 的复发风险。<sup>4</sup> 在更暴发性的病例中, 神经炎症、血脑屏障 (BBB) 通透性增加、星形胶质细胞肿胀、颅内高压和脑疝是主要的脑部病理表现。<sup>5,6</sup> 然而, 肝性脑病的确切细胞和分子机制仍知之甚少。目前的观点认为, 氨、谷氨酰胺以及肠道来源的神经毒性物质 (如硫醇、细胞因子、脂多糖和苯二氮草类药物) 在大脑中蓄积, 会激活小胶质细胞并触发一些重要的下游炎症信号传导, 诱导星形胶质细胞功能障碍, 扰乱大脑内稳态和神经变性, 最终导致肝性脑病的发作。<sup>7</sup> 治疗肝性脑病的药物处方通常是有效的, 但对于终末期肝病患者, 肝移植是治疗肝性脑病的唯一根治性治疗方法。<sup>8</sup> 在此, 我们对肝硬化合并肝性脑病患者脑组织的转录组数据进行了综合生物信息学研究, 通过多平台富集的生物学特征、脑区探索和转录后靶向分析, 来确定肝昏迷的所有机制。

## Methods

### 方法

## Identification of data sets

### 数据集的识别

Differentially expressed genes (DEGs) in the gene expression profiling of postmortem brain samples in cirrhotic patients with HE were identified from the public Gene Expression Omnibus (GEO) database (<https://www.ncbi.nlm.nih.gov/geo/>) and then analyzed with GEO2R Web tool as method described previously. The GEO is a public repository database for high-throughput gene expression measurements (ie, micro-array-based studies, RNA methylation profiling, genomic DNA and genome-protein interactions) supported by the National Center for Biotechnology Information.<sup>9,10</sup> Two data sets, namely, GSE41919 and GSE57193, were selected and analyzed for specified DEGs. In the last update of GEO, these data sets were only 2 accessible data sets that represented gene expression profiling of brain tissues in postmortem autopsy samples from patients with HE that protected GEO2R analysis. The GSE41919 data set was obtained from the cerebral cortex of 8 cirrhosis patients with HE and 8 healthy controls (<https://www.ncbi.nlm.nih.gov/geo/query/acc.cgi?acc=GSE41919>). The GSE57193 data set was prepared from the fusiform gyrus of 4 cirrhosis patients with HE and 4 healthy controls (<https://www.ncbi.nlm.nih.gov/geo/query/acc.cgi?acc=GSE57193>). We used the GEO2R Web tool to compare gene expression in cirrhotic data sets with healthy control to characterize DEGs ( $P < .05$ ). When log fold change (log FC) was more than 0 (positive value), genes were upregulated, and when log fold change was less than 0 (negative value), genes were downregulated.

11

从公共基因表达综合数据库 (GEO, <https://www.ncbi.nlm.nih.gov/geo/>) 中识别出肝硬化合并肝性脑病患者死后大脑样本基因表达谱中的差异表达基因 (DEGs), 然后按照之前描述的方法使用 GEO2R 网络工具进行分析。GEO 是一个由美国国家生物技术信息中心支持的公共存储数据库, 用于高通量基因表达测量 (即基于微阵列的研究、RNA 甲基化谱分析、基因组 DNA 和基因组 - 蛋白质相互作用)。<sup>9,10</sup> 选择了两个数据集, 即 GSE41919 和 GSE57193, 并对特定的差异表达基因进行分析。在 GEO 的最新更新中, 这两个数据集是仅有的两个可获取的、代表肝性脑病患者死后尸检样本脑组织基因表达谱且可进行 GEO2R 分析的数据集。GSE41919 数据集来自 8 例肝硬化合并肝性脑病患者和 8 例健康对照者的大脑皮层 (<https://www.ncbi.nlm.nih.gov/geo/query/acc.cgi?acc=GSE41919>)。GSE57193 数据集来自 4 例肝硬化合并肝性脑病患者和 4 例健康对照者的梭状回 (<https://www.ncbi.nlm.nih.gov/geo/query/acc.cgi?acc=GSE57193>)。我们使用 GEO2R 网络工具比较肝硬化数据集和健康对照的基因表达, 以表征差异表达基因 ( $P < .05$ )。当对数倍数变化 (log FC) 大于 0(正值) 时, 基因表达上调; 当对数倍数变化小于 0(负值) 时, 基因表达下调。<sup>11</sup>

---

Bioinformatics and Biology Insights Volume 17: 1-15 ©The Author(s) 2023 Article reuse guidelines: [sagepub.com/journals-permissions](https://sagepub.com/journals-permissions) DOI: 10.1177/11779322231155068 SSAGE

《生物信息学与生物学见解》第 17 卷:1 - 15 © 作者 (们)2023 文章再利用指南:[sagepub.com/journals-permissions](https://sagepub.com/journals-permissions) DOI: 10.1177/11779322231155068 SSAGE

## Construction of protein-protein interaction and network analysis of transcriptomic data

### 蛋白质 - 蛋白质相互作用的构建和转录组数据的网络分析

The STRING database (<https://string-db.org/>) was used to prepare protein-protein interaction networks for DEGs. All DEGs were uploaded into the STRING and proceeded after the selection of homo sapiens organisms for the construction of the genetic network. The STRING is a biological and an aniline Web tool platform that contains data from many organisms and computational algorithms to predict interactions between proteins or genes and is organized by Swiss Institute of Bioinformatics (SIB), Novo Nordisk Foundation Center Protein Research (CPR), and European Molecular Biology Laboratory (EMBL).<sup>12</sup> Afterward, a TSV file was downloaded and uploaded into Cytoscape version 3.7.0 to visualize the genetic network and analyzed main network parameters such as degree and betweenness centrality.<sup>13–15</sup> Top genes with more degree and greater betweenness centrality were considered as hub genes.<sup>16</sup>

使用 STRING 数据库 (<https://string-db.org/>) 为差异表达基因 (DEGs) 构建蛋白质 - 蛋白质相互作用网络。将所有 DEGs 上传到 STRING 数据库中, 选择智人 (homo sapiens) 生物体后进行基因网络的构建。STRING 是一个生物学和苯胺网络工具平台, 它包含来自许多生物体的数据和用于预测蛋白质或基因之间相互作用的计算算法, 由瑞士生物信息学研究所 (SIB)、诺和诺德基金会蛋白质研究中心 (CPR) 和欧洲分子生物学实验室 (EMBL) 组织维护。<sup>12</sup> 随后, 下载一个 TSV 文件并上传到 Cytoscape 3.7.0 版本中, 以可视化基因网络并分析主要的网络参数, 如度和介数中心性。<sup>13–15</sup> 度更高且介数中心性更大的顶级基因被视为枢纽基因。<sup>16</sup>

## Gene ontology, pathway, mammalian phenotype, cell type, and enrichment analysis of DEGs

### 差异表达基因的基因本体、通路、哺乳动物表型、细胞类型和富集分析

To investigate functional annotations in relation to obtained genes, biological processes enrichment analysis was conducted using ToppGene database (<https://toppgene.cchmc.org/>) for significant upregulated and downregulated genes separately. ToppGene-ToppFun is a computational online free-access tool for functional enrichment analysis of the candidate genes that included 16,930 and 322 annotations for biological processes and miRNA TargetScan, respectively, in the last update.<sup>17</sup> To get mechanistic insight into DEGs with  $P < .05$  from GEO, pathway enrichment analysis was performed using Enrichr database (<https://maayanlab.cloud/Enrichr/>).<sup>18,19</sup> Enrichr is a Web-based platform for analyzing candidate gene sets to predict common annotated biological features (ie, pathways, cellular type, phenotypes and transcription factors (TFs)).<sup>20</sup> For this purpose, 2 significant gene sets from DEGs (upregulated and downregulated) were separately submitted in Enrichr and proceeded through WikiPathway Web tool. Furthermore, to identify and compare the phenotype properties of each gene set, phenotype ontology was performed using Enrichr (Human Phenotype Ontology tool). Cellular component enrichment analysis was also conducted using Enrichr (Go cellular component tool) to reveal the main involved cellular components associated with upregulated and downregulated cerebral genes in HE. Also, PanglaoDB Augmented Web tool in Enrichr was

used to predict some specific cell types that may involve in cerebral damages following HE. The basic species for all enrichment were selected homo sapiens, and findings with  $P < .05$  were considered statistically significant.

为了研究与所获基因相关的功能注释, 分别使用 ToppGene 数据库 (<https://toppgene.cchmc.org/>) 对显著上调和下调的基因进行生物过程富集分析。ToppGene - ToppFun 是一个用于候选基因功能富集分析的免费在线计算工具, 在最新更新中, 它分别包含 16,930 条生物过程注释和 322 条 miRNA TargetScan 注释。<sup>17</sup> 为了深入了解来自 GEO 数据库且具有  $P < .05$  的 DEGs 的机制, 使用 Enrichr 数据库 (<https://maayanlab.cloud/Enrichr/>) 进行通路富集分析。<sup>18,19</sup> Enrichr 是一个基于网络的平台, 用于分析候选基因集以预测常见的注释生物学特征 (即通路、细胞类型、表型和转录因子 (TFs))。<sup>20</sup> 为此, 将 DEGs 中的 2 个显著基因集 (上调和下调) 分别提交到 Enrichr 中, 并通过 WikiPathway 网络工具进行分析。此外, 为了识别和比较每个基因集的表型特性, 使用 Enrichr (人类表型本体工具) 进行表型本体分析。还使用 Enrichr (Go 细胞成分工具) 进行细胞成分富集分析, 以揭示与肝性脑病 (HE) 中上调和下调的脑基因相关的主要细胞成分。此外, 还使用 Enrichr 中的 PanglaoDB 增强网络工具来预测可能参与 HE 后脑损伤的一些特定细胞类型。所有富集分析的基本物种均选择智人, 具有  $P < .05$  的结果被认为具有统计学意义。

## Time-series-specific tissue expression analysis

### 时间序列特异性组织表达分析

To identify time-series expression profiles across brain regions, we uploaded our target genes in a cell-type-specific expression analysis (CSEA) Web tool (<http://genetics.wustl.edu/jdlab/csea-tool-2/>). The CSEA is a Web-based platform to conduct brain-region-specific enrichment analysis for candidate genes that supports data from both mouse and human RNA-seq or/and microarray studies.<sup>21</sup> All significant upregulated and downregulated genes of DEGs were submitted in CSEA separately. Significant brain regions in different periods for input genes were described according to  $P$  value specificity index (pSI) and false discovery rate (FDR)-adjusted  $P$  value less than .05. Regions with lower pSI along with  $P$  value  $< .05$  were considered more important enriched.

为了识别跨脑区的时间序列表达谱, 我们将目标基因上传到细胞类型特异性表达分析 (CSEA) 网络工具 (<http://genetics.wustl.edu/jdlab/csea-tool-2/>) 中。CSEA 是一个基于网络的平台, 用于对候选基因进行脑区特异性富集分析, 支持来自小鼠和人类 RNA 测序或/和微阵列研究的数据。<sup>21</sup> 将 DEGs 中所有显著上调和下调的基因分别提交到 CSEA 中。根据  $P$  值特异性指数 (pSI) 和错误发现率 (FDR) 调整后的  $P$  值小于 0.05 来描述输入基因在不同时期的显著脑区。pSI 较低且  $P$  值  $< .05$  的区域被认为是更重要的富集区域。

## Transcription factors, microRNAs prediction and drug repurposing

### 转录因子、微小 RNA 预测和药物再利用

Transcription factor prediction analysis was performed using Enrichr through TRANSFAC and JASPAR PWMs Web tool to identify possible overlap between upregulated and down-regulated genes of DEGs and previously annotated TFs. To conduct microRNA (miRNA) target prediction annotations, we submitted target genes in the ToppGene database through the Target scan platform. Annotations that were predicted by more target genes

and presented lower  $P$  value were considered as main enrichments in all enrichment and target prediction analysis. Furthermore, a target-based drug discovery paradigm using ToppGene was performed to repurpose the main effective drugs or agents for cirrhosis-induced HE. To this goal, we uploaded our target genes in ToppGene-ToppFun and proceeded with drug discovery through Broad Institute Connectivity Map (CMAP), CTD, and Stitch in ToppGene (Figure 1). Statistical significance ( $P < .05$ ) was considered by a likelihood-ratio test with correction for FDR method to show comparison.

使用 Enrichr 通过 TRANSFAC 和 JASPAR PWMs 网络工具进行转录因子预测分析，以识别 DEGs 中上调和下调基因与先前注释的转录因子之间可能的重叠。为了进行微小 RNA(miRNA) 靶标预测注释，我们通过 Target scan 平台将目标基因提交到 ToppGene 数据库中。在所有富集和靶标预测分析中，由更多靶标基因预测且呈现较低  $P$  值的注释被视为主要富集。此外，使用 ToppGene 进行基于靶标的药物发现范式，以重新利用对肝硬化诱导的 HE 有效的主要药物或药剂。为此，我们将目标基因上传到 ToppGene - ToppFun 中，并通过 ToppGene 中的布罗德研究所连通性图谱 (CMAP)、CTD 和 Stitch 进行药物发现 (图 1)。通过似然比检验并采用 FDR 方法校正来确定统计学显著性 ( $P < .05$ )，以显示比较结果。

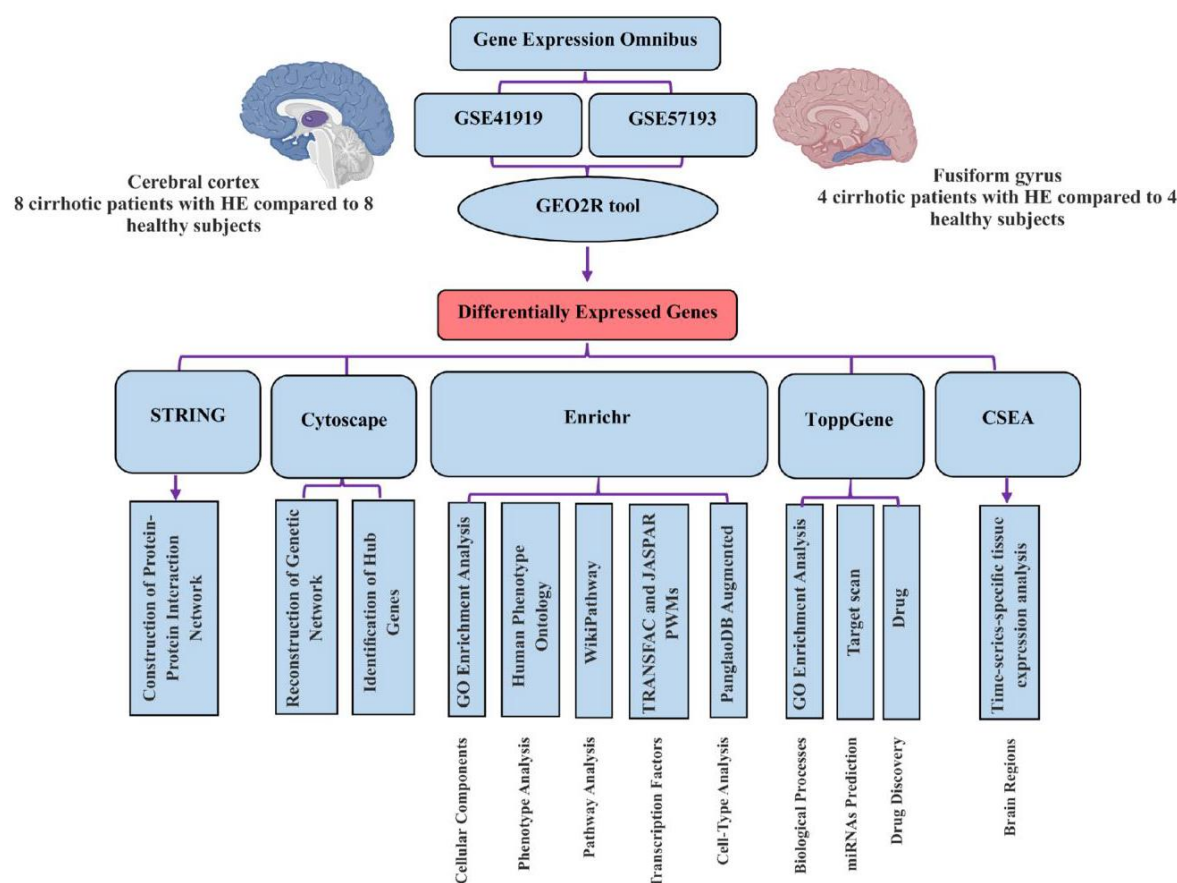


Figure 1. Schematic overview of conducted bioinformatics approach. Two data sets from postmortem brain samples of cirrhotic patients with HE were extracted from Gene Expression Omnibus. Differentially expressed genes were identified from both data sets using GEO2R Web tool. Different databases were also used to reveal new insight into molecular, cellular, and biological mechanisms as well as predict main probable therapeutic options in relation to HE. HE indicates hepatic encephalopathy.

图 1. 所采用的生物信息学方法的示意图。从基因表达综合数据库 (Gene Expression Omnibus) 中提取了两份来自肝性脑病 (HE) 肝硬化患者尸检脑样本的数据集。使用 GEO2R 网络工具从这两个数据集中识别出差异常表达基因。还利用不同的数据库来揭示分子、细胞和生物学机制的新见解，并预测与肝性脑病相关的主要可能治疗方案。HE 表示肝性脑病。

## Results

### 结果

## Identification of DEGs

### 差异表达基因 (DEGs) 的鉴定

We analyzed DEGs in 2 data sets using the GEO2R Web tool. Each expression profile consisted of 2 distinct gene sets of postmortem brain tissues from cirrhotic with HE and healthy control samples. The GSE41919 and GSE57193 data sets consisted of 4 and 453 significant DEGs, respectively. Among these, 3 and 271 known genes were significantly upregulated, while 1 and 182 known genes were significantly downregulated in GSE41919 and GSE57193, respectively (Figure 2 and Supplementary Table S1.). All consequent enrichment analysis and target predictions were conducted on total significant upregulated and downregulated from DEGs as our target genes, separately or totally according to enrichment goals.

我们使用 GEO2R 网络工具分析了两个数据集中的差异表达基因。每个表达谱由来自肝性脑病肝硬化患者和健康对照样本的两组不同的尸检脑组织基因集组成。GSE41919 和 GSE57193 数据集分别包含 4 个和 453 个显著差异表达基因。其中，在 GSE41919 和 GSE57193 数据集中，分别有 3 个和 271 个已知基因显著上调，1 个和 182 个已知基因显著下调 (图 2 和补充表 S1)。所有后续的富集分析和靶点预测均针对差异表达基因中显著上调和下调的基因作为目标基因进行，根据富集目标分别或整体进行分析。

## Construction of genetic network and analysis of network parameters

### 基因网络的构建和网络参数分析

To construct genetic networks and identify hub genes from our target genes, we used STRING and Cytoscape. Overall, there were 457 upregulated and downregulated genes in the Cytoscape. Among them, 58 genes (nodes) had no interactions. Network analysis using Cytoscape revealed that 10 hub genes such as epidermal growth factor receptor (EGFR), brain-derived neurotrophic factor (BDNF), Erb-b2 receptor tyrosine kinase 2 (ERBB2), glial fibrillary acidic protein (GFAP), aquaporin 4 (AQP4), solute carrier family 1 member 2 (SLC1A2), neurotrophic receptor tyrosine kinase 2 (NTRK2), neurotensin receptor 2 (NTSR2), Ras homolog family member C (RHOC), rhodopsin (RHO), paired box 6 (PAX6), and paxillin (PXN) had the biggest degrees and greatest betweenness centrality (Figure 3 and Table 1). EGFR (red circle node) related to 60 other genes in the current network and represented a bigger degree ( $D = 60$ ) and greater betweenness centrality ( $B = 0.22248615$ ). The main simple parameters of genetic networks included clustering coefficient ( $C_i$ ) = 0.181, network diameter ( $D$ ) = 10, network



centralization (C) = 0.135 , network density = 1.6% , and network heterogeneity (H) = 1.026 (Figure 3).

为了构建基因网络并从我们的目标基因中识别枢纽基因，我们使用了 STRING 和 Cytoscape 软件。总体而言，Cytoscape 中有 457 个上调和下调的基因。其中，58 个基因 (节点) 没有相互作用。使用 Cytoscape 进行的网络分析显示, 10 个枢纽基因, 如表皮生长因子受体 (EGFR)、脑源性神经营养因子 (BDNF)、Erb-b2 受体酪氨酸激酶 2(ERBB2)、胶质纤维酸性蛋白 (GFAP)、水通道蛋白 4(AQP4)、溶质载体家族 1 成员 2(SLC1A2)、神经营养因子受体酪氨酸激酶 2(NTRK2)、神经降压素受体 2(NTSR2)、Ras 同源家族成员 C(RHOC)、视紫红质 (RHO)、配对盒 6 (PAX6) 和桩蛋白 (PXN) 具有最大的度和最高的介数中心性 (图 3 和表 1)。EGFR(红色圆圈节点) 在当前网络中与 60 个其他基因相关，代表了更大的度 (D = 60) 和更高的介数中心性 (B = 0.22248615)。基因网络的主要简单参数包括聚类系数 (Ci) = 0.181、网络直径 (D) = 10、网络中心化程度 (C) = 0.135、网络密度 = 1.6% 和网络异质性 (H) = 1.026 (图 3)。

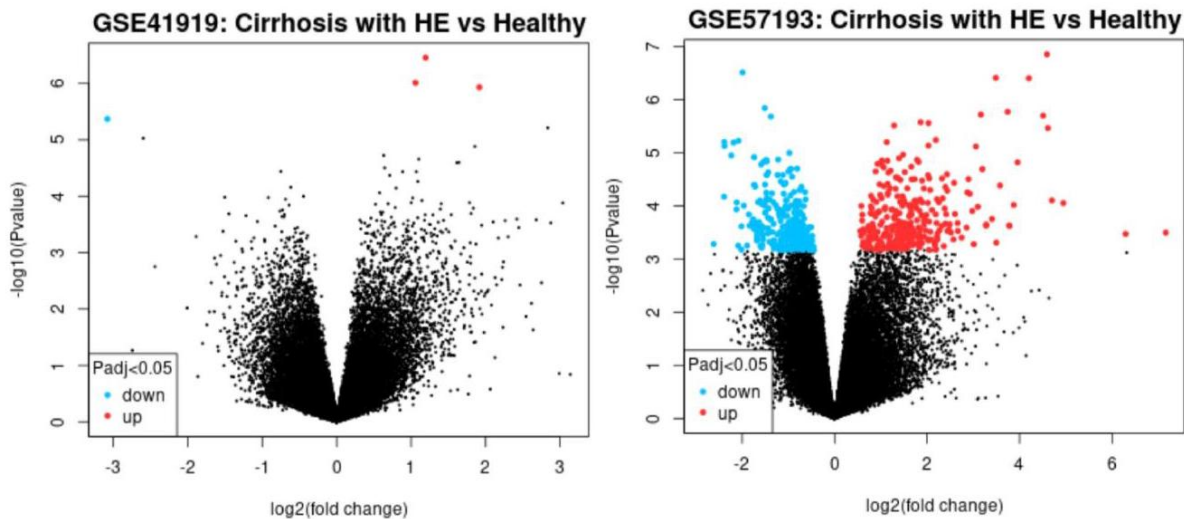


Figure 2. Volcano plots of significant differentially expressed genes in cerebral tissues from cirrhosis-induced HE patients. Two transcriptomic data sets were extracted from public Gene Expression Omnibus and then analyzed using GEO2R Web tool to identify regulation patterns of significant genes. When log2fold change was positive, genes were up-regulated (red nodes), and when it was negative, genes were downregulated (blue nodes). HE indicates hepatic encephalopathy.

图 2. 肝硬化诱发肝性脑病患者脑组织中显著差异表达基因的火山图。从公共基因表达综合数据库中提取了两个转录组数据集，然后使用 GEO2R 网络工具进行分析，以确定显著基因的调控模式。当 log2 倍数变化为正时，基因上调 (红色节点)；当为负时，基因下调 (蓝色节点)。HE 表示肝性脑病。

## Biological insights of target genes

### 目标基因的生物学见解

Biological process enrichment analysis showed that circulatory system development, organic acid catabolic process, lipid metabolic process, carboxylic acid catabolic process, lipid modification, lipid oxidation, anatomical structure formation involved in morphogenesis, cell adhesion, glial cell differentiation, and regulation of actin cytoskeleton organization were significantly enriched for upregulated genes (Figure 4A), whereas neuron projection development, cellular component morphogenesis, neuron projection morphogenesis, plasma membrane-bounded cell projection morphogenesis, cell projection morphogenesis, cell part morphogenesis, and neuron development were enriched for downregulated genes (Figure 4B). Pathway analysis revealed that fatty acid beta-oxidation WP143, mitochondrial LC-Fatty acid beta-oxidation WP368, cerebral organic acidurias WP4519, and regulation of actin cytoskeleton WP51 were significantly annotated for upregulated genes (Figure 4C), whereas serotonin receptor 2 and ETS-like protein (ELK)- serum response factor (SRF)/GATA Binding Protein 4 (GATA4) signaling WP732, vitamin A, carotenoid metabolism WP716, G protein-coupled receptors (GPCRs), class A rhodopsin-like WP455, and p38 mitogen-activated protein kinase (MAPK) signaling pathway WP400 were significantly enriched for downregulated genes (Figure 4D).

生物过程富集分析表明，循环系统发育、有机酸分解代谢过程、脂质代谢过程、羧酸分解代谢过程、脂质修饰、脂质氧化、参与形态发生的解剖结构形成、细胞黏附、神经胶质细胞分化以及肌动蛋白细胞骨架组织的调节等生物过程在上调基因中显著富集(图 4A)；而神经元突起发育、细胞成分形态发生、神经元突起形态发生、质膜包被的细胞突起形态发生、细胞突起形态发生、细胞部分形态发生以及神经元发育等生物过程在下调基因中富集(图 4B)。通路分析显示，脂肪酸  $\beta$ -氧化(WP143)、线粒体长链脂肪酸  $\beta$ -氧化(WP368)、脑有机酸尿症(WP4519)以及肌动蛋白细胞骨架的调节(WP51)等通路在上调基因中显著注释(图 4C)；而血清素受体 2 和 ETS 样蛋白(ELK)-血清反应因子(SRF)/GATA 结合蛋白 4(GATA4) 信号通路(WP732)、维生素 A 和类胡萝卜素代谢(WP716)、A 类视紫红质样 G 蛋白偶联受体(GPCRs, WP455)以及 p38 丝裂原活化蛋白激酶(MAPK) 信号通路(WP400)等通路在下调基因中显著富集(图 4D)。

Gene-phenotype prediction analysis provided abnormality of dicarboxylic acid metabolism (HP:0010995), dicarboxylic aciduria (HP:0003215), hyperammonemia (HP:0001987), myoglobinuria (HP:0002913), and bradycardia (HP:0001662) as significant enriched human phenotypes in relation to upregulated genes (Figure 5A), whereas some phenotypes such as inability to walk (HP:0002540), progressive inability to walk (HP:0002505), akinesia (HP:0002304), fatigable weakness (HP:0003473), and abnormality of the neuromuscular junction (HP:0003398) were significantly annotated for downregulated genes (Figure 5B). Furthermore, cell-type-specific enrichment analysis showed that astrocytes, Bergmann glia, oligodendrocytes, Schwann cells, and satellite glial cells were the most important affected cells in relation to upregulated genes (Figure 5C), whereas photoreceptor cells, pyramidal cells, retinal ganglion cells, and neuroblasts were the most significantly involved cell types in relation to downregulated genes (Figure 5D). Also, cellular component enrichment revealed that lipid droplet (GO:0005811), focal adhesion (GO:0005925), cell-substrate junction (GO:0030055), astrocyte projection (GO:0097449), and sodium:potassium-exchanging ATPase complex (GO:0005890) were the main disrupted cellular elements that were enriched by upregulated gene (Figure 5E), whereas neuron projection (GO:0043005), sarcoplasmic reticulum membrane (GO:0033017), secretory vesicle (GO:0099503), voltage-gated potassium channel complex (GO:0008076), and ciliary membrane (GO:0060170) were the most affected cellular components that were annotated for downregulated genes (Figure 5F).

基因 - 表型预测分析显示, 二羧酸代谢异常 (HP:0010995)、二羧酸尿症 (HP:0003215)、高氨血症 (HP:0001987)、肌红蛋白尿症 (HP:0002913) 以及心动过缓 (HP:0001662) 等人类表型与上调基因显著富集相关 (图 5A); 而一些表型, 如不能行走 (HP:0002540)、进行性不能行走 (HP:0002505)、运动不能 (HP:0002304)、易疲劳性肌无力 (HP:0003473) 以及神经肌肉接头异常 (HP:0003398) 等在下调基因中显著注释 (图 5B)。此外, 细胞类型特异性富集分析表明, 星形胶质细胞、伯格曼胶质细胞、少突胶质细胞、施万细胞和卫星胶质细胞是与上调基因相关的受影响最显著的细胞类型 (图 5C); 而光感受器细胞、锥体细胞、视网膜神经节细胞和神经母细胞是与下调基因相关的最显著涉及的细胞类型 (图 5D)。同时, 细胞成分富集分析显示, 脂滴 (GO:0005811)、黏着斑 (GO:0005925)、细胞 - 基质连接 (GO:0030055)、星形胶质细胞突起 (GO:0097449) 以及钠钾交换 ATP 酶复合物 (GO:0005890) 是上调基因富集的主要受干扰细胞成分 (图 5E); 而神经元突起 (GO:0043005)、肌质网膜 (GO:0033017)、分泌小泡 (GO:0099503)、电压门控钾离子通道复合物 (GO:0008076) 以及纤毛膜 (GO:0060170) 是下调基因注释的受影响最显著的细胞成分 (图 5F)。

## Time-series-specific tissue expression analysis

### 时间序列特异性组织表达分析

Due to the dynamic nature of gene expression at different stages of life, we conducted a time-specific tissue expression analysis for total upregulated and downregulated genes. We displayed that our target genes significantly enriched some functional brain regions such as thalamus, striatum, cortex, amygdale, and hippocampus (Figure 6A). Time-specific expression analysis revealed that target genes were strongly expressed in the thalamus at different periods of life, including neonatal early infancy, late infancy, early childhood, mid-late childhood, adolescence, and young adulthood (Figure 6B).

由于基因表达在生命不同阶段具有动态特性, 我们对全部上调和下调基因进行了时间特异性组织表达分析。结果显示, 我们的目标基因在一些功能性脑区显著富集, 如丘脑、纹状体、皮质、杏仁核和海马体 (图 6A)。时间特异性表达分析表明, 目标基因在生命的不同时期, 包括新生儿早期、婴儿晚期、幼儿期、儿童中后期、青春期和青年期, 在丘脑中强烈表达 (图 6B)。

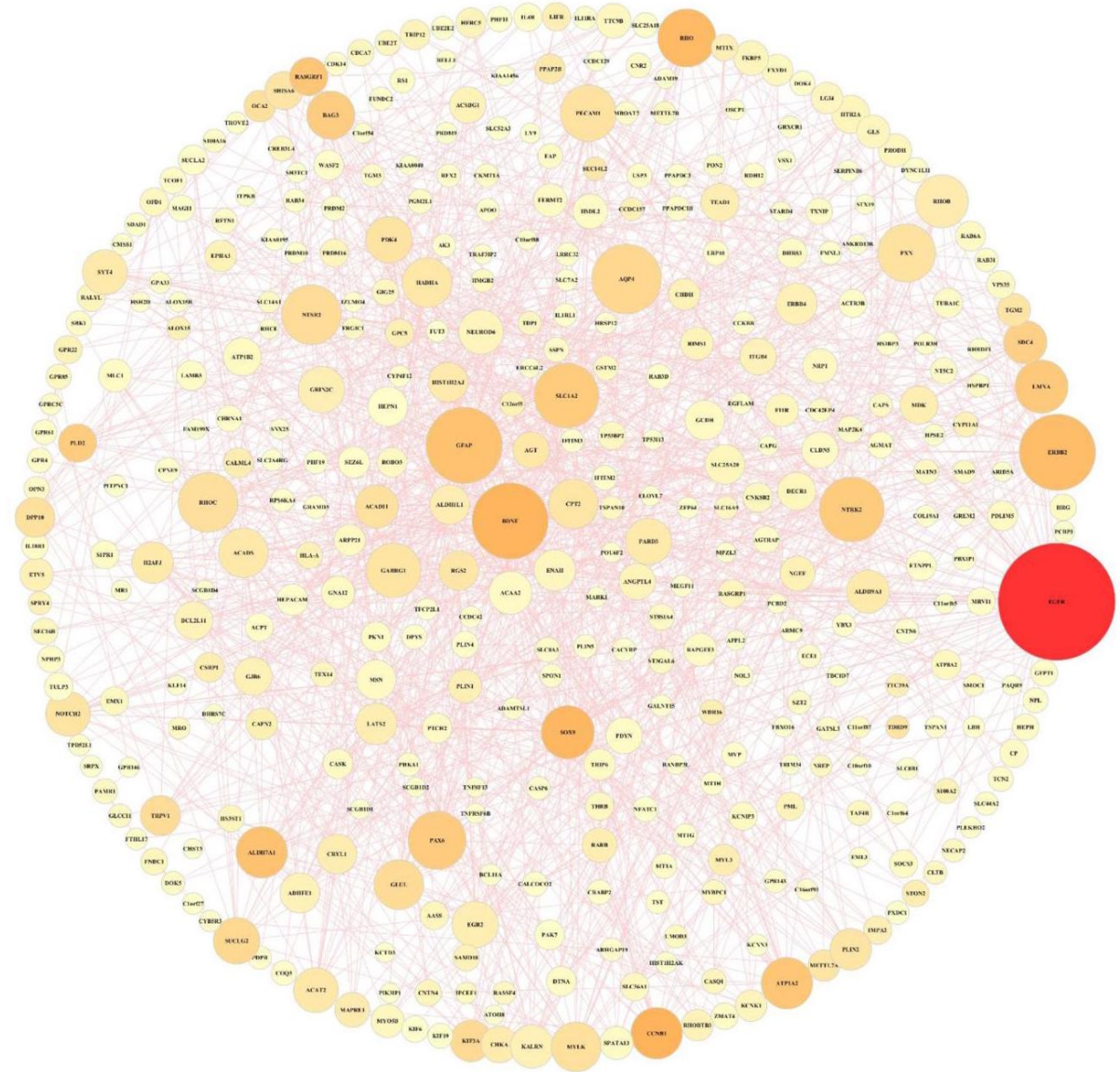


Figure 3. Genetic network of targeted significant DEGs from the brain of cirrhosis-induced HE patients. The network consists of 399 interacted nodes. In the current network, 12 genes such as EGFR, BDNF, ERBB2, GFAP, AQP4, SLC1A2, NTRK2, NTSR2, RHOC, RHOC, RHO, PAX6, and PXN were more centralized and considered as hub genes. Each node is illustrated according to its network parameters. The size and color of nodes are adjusted with their degrees and betweenness centrality, respectively. Large nodes represent a bigger degree, and red and dark orange nodes indicate greater betweenness centrality. DEGs indicate differentially expressed genes; HE, hepatic encephalopathy.

图 3. 肝硬化诱发肝性脑病 (HE) 患者大脑中靶向显著差异表达基因 (DEGs) 的遗传网络。该网络由 399 个相互作用的节点组成。在当前网络中, 如表皮生长因子受体 (EGFR)、脑源性神经营养因子 (BDNF)、人表皮生长因子受体 2(ERBB2)、胶质纤维酸性蛋白 (GFAP)、水通道蛋白 4(AQP4)、溶质载体家族 1 成员 2(SLC1A2)、神经营养因子受体酪氨酸激酶 2(NTRK2)、神经降压素受体 2(NTSR2)、Rho 相关卷曲螺旋形成蛋白激酶 C(RHOC)、Rho 相关卷曲螺旋形成蛋白激酶 C(RHOC)、Rho 蛋白 (RHO)、配对盒基因 6(PAX6) 和桩蛋白 (PXN) 等 12 个基因更为中心化, 被视为枢纽基因。每个节点根据其网络参数进行展示。节点的大小和颜色分别根据其度和介数中心性进行调整。大节点表示度更大, 红色和深橙色节点表示介数中心性更高。DEGs 表示差异表达基因; HE 表示肝性脑病。

## Drug repurposing

### 药物再利用

Gene-drug interaction prediction was conducted to repurpose some effective drugs or small molecules for target genes using ToppGene through CTD, Stitch, and Broad Institute Connectivity Map tools. Thirty-nine drugs or agents such as flufenamic acid ( $P = 2.70E - 09$  ; predicted by 20 input genes; gene count (GC = 20) ), troglitazone ( $P = 4.56E - 09$ ; GC = 59) , zoledronic acid ( $P = 3.00E - 08$ ; GC = 61) , raloxifene hydrochloride ( $P = 6.50E - 08$ ; GC = 42) , buspirone ( $P = 3.06E - 07$ ; GC = 33) , acetylcysteine ( $P = 3.29E - 07$ ; GC = 38) , calphostin C ( $P = 5.30E - 07$ ; GC = 26) , ketamine ( $P = 6.13E - 07$ ; GC = 38) , gamma-aminobutyric acid ( $P = 9.75E - 07$ ; GC = 27) , vanadates ( $P = 2.42E - 06$ ; GC = 51) , rosiglitazone ( $P = 2.99E - 06$ ; GC = 58) , retinoic acid ( $P = 3.43E - 06$  ; GC = 14) , trichostatin A ( $P = 4.59E - 06$  ; GC = 14) , vancomycin ( $P = 4.84E - 06$ ; GC = 39) , haloperidol ( $P = 5.02E - 06$ ; GC = 21) , cocaine ( $P = 6.82E - 06$ ; GC = 50) , MK-801 ( $P = 7.53E - 06$ ; GC = 19) , leflunomide ( $P = 8.70E - 06$ ; GC = 36) , cytarabine ( $P = 9.22E - 06$ ; GC = 29) , clozapine ( $P = 1.15E - 05$ ; GC = 22) , doxorubicin ( $P = 1.28E - 05$ ; GC = 61) , thapsigargin ( $P = 1.47E - 05$ ; GC = 50) , demecol-cine ( $P = 3.11E - 05$ ; GC = 36) , amiodarone ( $P = 3.23E - 05$ ; GC = 52) , fluorouracil ( $P = 3.77E - 05$ ; GC = 49) , and panto-gab ( $P = 6.96E - 05$ ; GC = 27) were predicted and identified for upregulated and downregulated gene expression of cirrhosis patients with HE (Figure 7A). Among predicted results, 6 agents (ie, flufenamic acid, troglitazone, zoledronic acid, raloxifene hydrochloride, buspirone and acetylcysteine) had the lowest  $P$  value and were classified as more significant agents (green nodes in Figure 7B). Furthermore, 7 agents (ie, zoledronic acid, doxorubicin, troglitazone, rosiglitazone, amiodarone, vanadates, and cocaine) were predicted by a greater number of input genes (larger nodes in Figure 7B).

通过 CTD、Stitch 和布罗德研究所连通性图谱 (Broad Institute Connectivity Map) 工具, 使用 ToppGene 进行基因 - 药物相互作用预测, 为目标基因重新利用一些有效的药物或小分子。预测并鉴定出 39 种药物或药剂, 如氟芬那酸 ( $P = 2.70E - 09$  (由 20 个输入基因预测; 基因计数 (GC = 20) )、曲格列酮 ( $P = 4.56E - 09$ ; GC = 59)、唑来膦酸 ( $P = 3.00E - 08$ ; GC = 61)、盐酸雷洛昔芬 ( $P = 6.50E - 08$ ; GC = 42)、丁螺环酮 ( $P = 3.06E - 07$  ( GC = 33 )、乙酰半胱氨酸 ( $P = 3.29E - 07$ ; GC = 38)、钙感光蛋白 C ( $P = 5.30E - 07$ ; GC = 26)、氯胺酮 ( $P = 6.13E - 07$  ( GC = 38 )、 $\gamma$ -氨基丁酸 ( $P = 9.75E - 07$  ( GC = 27 )、钒酸盐 ( $P = 2.42E - 06$ ; GC = 51)、罗格列酮 ( $P = 2.99E - 06$ ; GC = 58)、维甲酸 ( $P = 3.43E - 06$  ( GC = 14) )、曲古抑菌素 A ( $P = 4.59E - 06$  ( GC = 14 )、万古霉素 ( $P = 4.84E - 06$ ; GC = 39)、氟哌啶醇 ( $P = 5.02E - 06$ ; GC = 21)、可卡因 ( $P = 6.82E - 06$ ; GC = 50)、MK - 801 ( $P = 7.53E - 06$ ; GC = 19)、来氟米特 ( $P = 8.70E - 06$ ; GC = 36)、阿糖胞苷 ( $P = 9.22E - 06$ ; GC = 29)、氯氮平 ( $P = 1.15E - 05$ ; GC = 22)、多柔比星 ( $P = 1.28E - 05$  ( GC = 61 )、毒胡萝卜素 ( $P = 1.47E - 05$ ; GC = 50)、秋水仙胺 ( $P = 3.11E - 05$ ; GC = 36)、胺碘酮 ( $P = 3.23E - 05$  ( GC = 52 )、氟尿嘧啶 ( $P = 3.77E - 05$ ; GC = 49) 和泛加巴 ( $P = 6.96E - 05$ ; GC = 27) , 这些药物或药剂可用于肝性脑病 (HE) 肝硬化患者基因表达上调和下调的治疗 (图 7A)。在预测结果中, 6 种药剂 (即氟芬那酸、曲格列酮、唑来膦酸、盐酸雷洛昔芬、丁螺环酮和乙酰半胱氨酸) 的  $P$  值最低, 被归类为更显著的药剂 (图 7B 中的绿色节点)。此外, 7 种药剂 (即唑来膦酸、多柔比星、曲格列酮、罗格列酮、胺碘酮、钒酸盐和可卡因) 由更多数量的输入基因预测得出 (图 7B 中的较大节点)。

Table 1. Specific cerebral hub genes associated with cirrhosis-induced HE based on network analysis using Cytoscape.

表 1. 基于使用 Cytoscape 进行网络分析确定的与肝硬化诱发的肝性脑病 (HE) 相关的特定大脑枢纽基因。

INDEX	GENE SYMBOL	GENE FULL NAME	DEGREE	BETWEENNESS CENTRALITY
1.	EGFR	Epidermal growth factor receptor	60	0.22248615
2.	BDNF	Brain-derived neurotrophic factor	35	0.05149659
3.	ERBB2	Erb-b2 receptor tyrosine kinase 2	35	0.04581279
4.	GFAP	Glial fibrillary acidic protein	35	0.04277803
5.	AQP4	Aquaporin 4	31	0.02808841
6.	SLC1A2	Solute carrier family 1 member 2	28	0.03655976
7.	NTRK2	Neurotrophic receptor tyrosine kinase 2	28	0.03655484
8.	NTSR2	Neurotensin receptor 2	25	0.02365894
9.	RHOC	Ras homolog family member C	25	0.02198101
10.	RHO	Rhodopsin	24	0.04789389
11.	PAX6	Paired box 6	24	0.03581797
12.	PXN	Paxillin	24	0.02051758

索引	基因符号	基因全称	度	介数中心性
1.	EGFR(表皮生长因子受体)	表皮生长因子受体	60	0.22248615
2.	BDNF(脑源性神经营养因子)	脑源性神经营养因子	35	0.05149659
3.	ERBB2(Erb-b2 受体酪氨酸激酶 2)	Erb-b2 受体酪氨酸激酶 2	35	0.04581279
4.	GFAP(胶质纤维酸性蛋白)	胶质纤维酸性蛋白	35	0.04277803
5.	AQP4(水通道蛋白 4)	水通道蛋白 4	31	0.02808841
6.	SLC1A2(溶质载体家族 1 成员 2)	溶质载体家族 1 成员 2	28	0.03655976
7.	NTRK2(神经营养受体酪氨酸激酶 2)	神经营养受体酪氨酸激酶 2	28	0.03655484
8.	NTSR2(神经降压素受体 2)	神经降压素受体 2	25	0.02365894
9.	RHOC(Ras 同源家族成员 C)	Ras 同源家族成员 C	25	0.02198101
10.	RHO(视紫红质)	视紫红质	24	0.04789389
11.	PAX6(配对盒 6)	配对盒 6	24	0.03581797
12.	PXN(桩蛋白)	桩蛋白	24	0.02051758

## Transcription factor prediction and targeted miRNAs

### 转录因子预测与靶向微小 RNA

Since gene expression is strongly regulated by post-transcriptional processes and TFs, we conducted TFs and microRNAs (miRNAs) target prediction analysis for both upregulated and downregulated genes separately through Enrichr and ToppGene databases, respectively. We predicted 7 significant TFs such as SMAD family member 4, mothers against decapentaplegic homolog 4 (SMAD4); nuclear receptor subfamily 5 group A member 2 (NR5A2); nuclear factor I A (NFIA); upstream binding transcription factor (UBTF); hepatocyte nuclear factor 1-alpha (HNF1A); MAX interactor 1, dimerization protein (MXI1); and MAPK14 and 10 important miRNAs such as hsa-miR-325-3p, hsa-miR-124-3p.1, hsa-miR-495-3p, hsa-miR-24-3p, hsa-miR-133a-3p.1, hsa-miR-506-3p, hsa-miR-124-3p.2, hsa-miR-497-5p, hsa-miR-16-5p, and hsa-miR-15a-5p for genes that were upregulated in brain tissue of HE patients. We also predicted 7 significant TFs such as transcription factor 4 (TCF4), TEA domain transcription factor 2 (TEAD2), HNF1A, myocyte enhancer factor 2A (MEF2A), jun proto-oncogene, AP-1 transcription factor subunit (JUN), nuclear factor I C (NFIC) and SRF and 10 important miRNAs such as hsa-miR-27b-3p, hsa-miR-27a-3p, hsa-miR-23a-3p, hsa-miR-23b-3p, hsa-miR-23c, hsa-miR-124-3p.1, hsa-miR-30e-5p, hsa-miR-30a-5p, hsa-miR-30d-5p, and hsa-miR-30b-5p for down-regulated genes (Table 2).



由于基因表达受到转录后过程和转录因子 (TFs) 的严格调控, 我们分别通过 Enrichr 和 ToppGene 数据库, 对上调和下调基因进行了 TFs 和微小 RNA(miRNAs) 靶标预测分析。我们预测出 7 个显著的 TFs, 如 SMAD 家族成员 4(SMAD4, 即抗果蝇畸形翅同源物 4)、核受体亚家族 5A 组 2 号成员 (NR5A2)、核因子 I A(NFIA)、上游结合转录因子 (UBTF)、肝细胞核因子 1- $\alpha$ (HNF1A)、MAX 相互作用蛋白 1(MXI1, 一种二聚化蛋白)、MAPK14; 以及 10 个重要的 miRNAs, 如 hsa - miR - 325 - 3p、hsa - miR - 124 - 3p.1、hsa - miR - 495 - 3p、hsa - miR - 24 - 3p、hsa - miR - 133a - 3p.1、hsa - miR - 506 - 3p、hsa - miR - 124 - 3p.2、hsa - miR - 497 - 5p、hsa - miR - 16 - 5p 和 hsa - miR - 15a - 5p, 这些是肝性脑病 (HE) 患者脑组织中上调基因对应的。我们还预测出 7 个显著的 TFs, 如转录因子 4(TCF4)、TEA 结构域转录因子 2(TEAD2)、HNF1A、肌细胞增强因子 2A(MEF2A)、jun 原癌基因 (JUN, AP - 1 转录因子亚基)、核因子 I C(NFIC) 和 SRF; 以及 10 个重要的 miRNAs, 如 hsa - miR - 27b - 3p、hsa - miR - 27a - 3p、hsa - miR - 23a - 3p、hsa - miR - 23b - 3p、hsa - miR - 23c、hsa - miR - 124 - 3p.1、hsa - miR - 30e - 5p、hsa - miR - 30a - 5p、hsa - miR - 30d - 5p 和 hsa - miR - 30b - 5p, 这些是下调基因对应的 (表 2)。

## Discussion

### 讨论

Hepatic encephalopathy is a serious and common complication in patients with end-stage liver disease. The molecular and cellular mechanisms of HE are not fully settled.<sup>22</sup> Microarray technology reveals DEGs and provides abnormalities of gene expression patterns in the whole genome. Therefore, these expression abnormalities can be useful for disclosing the mechanisms of diseases. Here, we combined 2 transcriptomic data sets from cerebral tissues of cirrhotic patients with HE and analyzed them to not only examine DEGs but also open new windows to disclose the pathophysiology of HE and possible new therapeutic options through an integrative bioinformatics approach.

肝性脑病是终末期肝病患者常见且严重的并发症。HE 的分子和细胞机制尚未完全明确。<sup>22</sup> 微阵列技术可揭示差异表达基因 (DEGs), 并呈现全基因组范围内基因表达模式的异常。因此, 这些表达异常有助于揭示疾病的发病机制。在此, 我们整合了两份来自肝硬化合并 HE 患者脑组织的转录组数据集, 并进行分析, 不仅检测了 DEGs, 还通过综合生物信息学方法为揭示 HE 的病理生理学机制和探索可能的治疗方案开辟了新途径。

In this study, 274 genes were upregulated and 183 genes were downregulated from both GSE41919 and GSE57193 data sets. Protein-protein interaction network analysis identified 12 hub genes such as EGFR, BDNF, ERBB2, GFAP, AQP4, SLC1A2, NTRK2, NTSR2, RHOC, RHO, PAX6, and PXN as centralized and significant genes in the genetic network (Table 1).

在本研究中, 从 GSE41919 和 GSE57193 数据集中筛选出 274 个上调基因和 183 个下调基因。蛋白质 - 蛋白质相互作用网络分析确定了 12 个枢纽基因, 如表皮生长因子受体 (EGFR)、脑源性神经营养因子 (BDNF)、人表皮生长因子受体 2(ERBB2)、胶质纤维酸性蛋白 (GFAP)、AQP4, SLC1A2, NTRK2, NTSR2, RHOC, RHO, PAX6 和 PXN, 它们是基因网络中处于核心地位的重要基因 (表 1)。



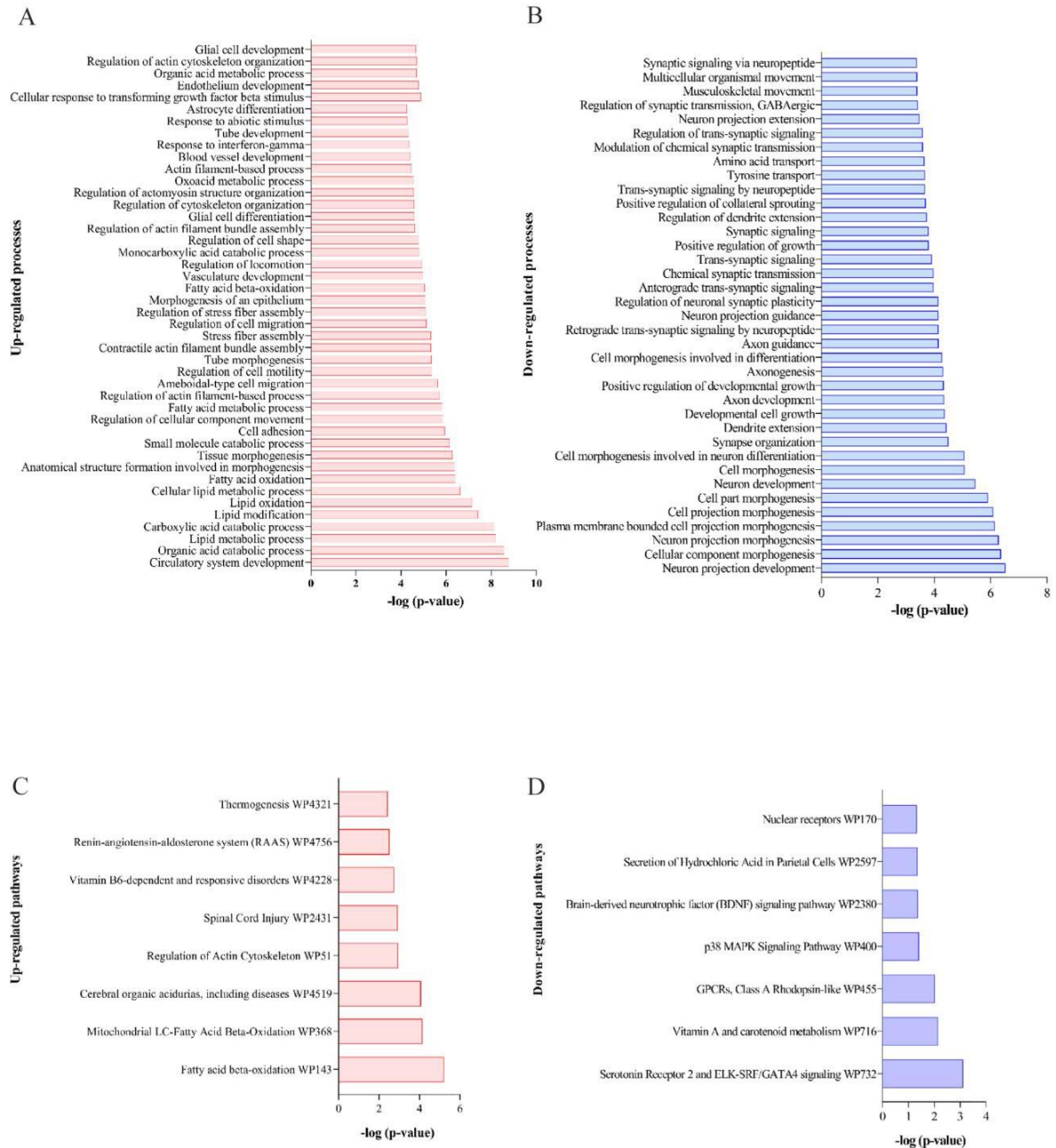


Figure 4. Biological process and pathway enrichment analysis for significant DEGs. Significant biological processes were enriched for upregulated (A) and downregulated (B) target genes. Main involved pathways annotated for upregulated (C) and downregulated (D) target genes. All results are adjusted based on  $P$  value and presented as  $-\log(P\text{ value})$  on the horizontal axis. DEGs indicate differentially expressed genes.

图 4. 显著差异表达基因的生物过程和通路富集分析。上调 (A) 和下调 (B) 靶基因富集的显著生物过程。上调 (C) 和下调 (D) 靶基因注释的主要涉及通路。所有结果均基于  $P$  值进行调整，并以  $-\log(P\text{ 值})$  的形式在横轴上呈现。DEGs 表示差异表达基因。

The EGFR (epidermal growth factor receptor) is a transmembrane protein and a member of the ErbB family receptors. Activation of receptors by EGF through downstream signaling molecules and cascades such as MAPK and Akt induces DNA synthesis, cell proliferation, and migration.<sup>23</sup> These receptors mediated liver fibrogenesis

and hepatocarcinogenesis processes in animal models of cirrhosis and HE.<sup>24–26</sup> These receptors also played an important role in the progress of nonalcoholic fatty liver disease as a risk factor for the development of cirrhosis.<sup>27</sup> Polymorphism in *EGFR* was also associated with risk of hepatocellular carcinoma in cirrhotic subjects<sup>28</sup> and also circulatory levels of these proteins were correlated with the severity of disease in hepatocellular carcinoma patients.<sup>29</sup> Activation of *EGFR* in ammonia-exposed astrocytes as in vitro model of HE mediates ammonia-induced astrocyte swelling.<sup>30</sup> Furthermore, in azoxymethane-induced HE mice, activation of EGFR through p38 MAPK/NF  $\kappa$  B may involve in the disruption of the BBB and progression of cerebral edema.<sup>31</sup>

表皮生长因子受体 (EGFR) 是一种跨膜蛋白, 属于 ErbB 家族受体成员。表皮生长因子 (EGF) 通过下游信号分子和级联反应 (如丝裂原活化蛋白激酶 (MAPK) 和蛋白激酶 B(Akt)) 激活受体, 可诱导 DNA 合成、细胞增殖和迁移。<sup>23</sup> 在肝硬化和肝性脑病 (HE) 动物模型中, 这些受体介导了肝纤维化和肝癌发生过程。<sup>24–26</sup> 作为肝硬化发生的危险因素, 这些受体在非酒精性脂肪性肝病进展中也发挥着重要作用。<sup>27</sup> *EGFR* 的多态性也与肝硬化患者患肝细胞癌的风险相关<sup>28</sup>, 并且这些蛋白的循环水平与肝细胞癌患者的疾病严重程度相关。<sup>29</sup> 在作为肝性脑病体外模型的氨暴露星形胶质细胞中, *EGFR* 的激活介导了氨诱导的星形胶质细胞肿胀。<sup>30</sup> 此外, 在偶氮甲烷诱导的肝性脑病小鼠中, 通过 p38 丝裂原活化蛋白激酶 (MAPK)/核因子  $\kappa$  B 激活表皮生长因子受体可能参与血脑屏障 (BBB) 的破坏和脑水肿的进展。<sup>31</sup>

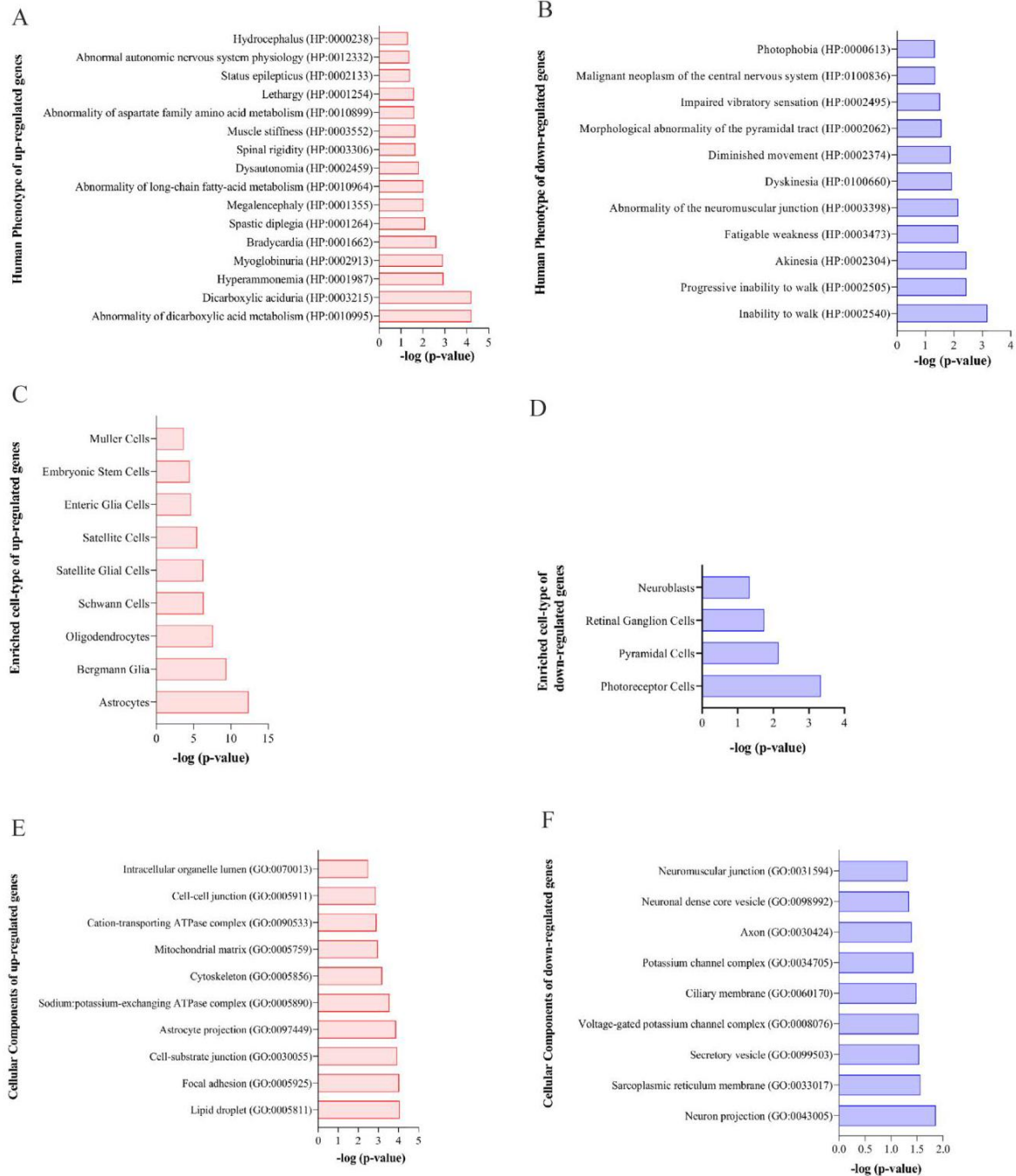


Figure 5. Human profiling, cell type, and cellular component enrichment analysis for significant DEGs. Human phenotype enrichment annotated for cerebral upregulated (A) and downregulated (B) HE genes. Result of cell type prediction for upregulated (C) and downregulated (D) HE genes using Enrichr database. Enriched cellular components for cerebral upregulated (E) and downregulated (F) HE genes. All results are adjusted based on P value and presented as  $-\log(P \text{ value})$  on the horizontal axis. DEGs indicate differentially expressed genes; HE, hepatic encephalopathy.

图 5. 显著差异表达基因 (DEGs) 的人类特征分析、细胞类型分析和细胞成分富集分析。对大脑上调 (A) 和下调 (B) 的肝性脑病相关基因进行人类表型富集注释。使用 Enrichr 数据库对上调 (C) 和下调 (D) 的肝性脑病相关基因进行细胞类型预测的结果。大脑上调 (E) 和下调 (F) 的肝性脑病相关基因的富集细胞成分。所有结果均基于 P 值进行调整, 并在横轴上以  $-\log(P \text{ 值})$  表示。DEGs 表示差异表达基因; HE 表示肝性脑病。

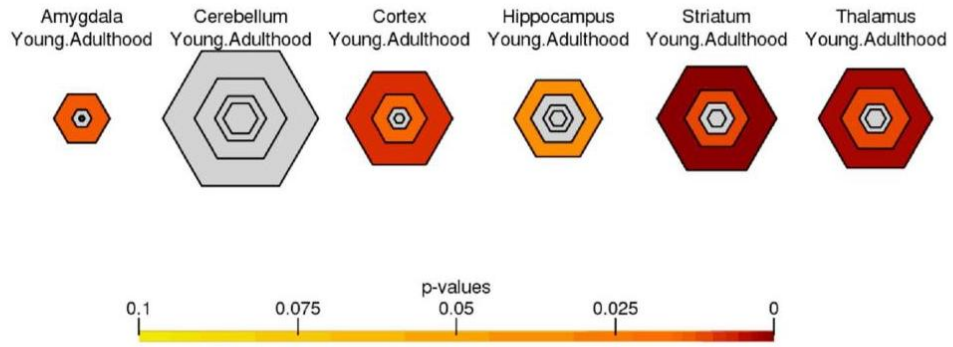
The second hub gene *BDNF* is a neurotrophin growth factor that is involved in many vital developmental processes of

第二个枢纽基因 *BDNF* 是一种神经营养生长因子, 参与中枢神经系统 (CNS) 许多重要的发育过程

central nervous system (CNS), especially synaptogenesis, neurogenesis, synapse stability, and neurotransmitter signaling.<sup>32</sup> Abnormal expression of *BDNF* in cirrhosis-induced HE was mentioned previously in clinical, animal, and in vitro culture studies. The level of *BDNF* was significantly decreased in serum samples of patients with cirrhosis due to biliary atresia and hepatitis.<sup>33,34</sup> Recently, a human study by Stawicka et al<sup>35</sup> presented serum levels of *BDNF* were decreased in cirrhosis patients with HE and introduced it as a diagnostic marker for HE. Furthermore, the protein and expression levels of *BDNF* were significantly decreased in the brain tissues of hyperammonemic animal models of HE.<sup>36–40</sup> Also, the *BDNF*-induced functional morphological changes of astrocytes were disrupted when cultures were exposed to ammonia.<sup>41</sup>

, 尤其是突触发生、神经发生、突触稳定性和神经递质信号传导。<sup>32</sup> 先前在临床、动物和体外培养研究中均提及肝硬化诱导的肝性脑病中脑源性神经营养因子 (BDNF) 表达异常。在因胆道闭锁和肝炎导致肝硬化的患者血清样本中, *BDNF* 的水平显著降低。<sup>33,34</sup> 最近, Stawicka 等人<sup>35</sup> 的一项人体研究表明, 肝性脑病肝硬化患者血清中 *BDNF* 的水平降低, 并将其作为肝性脑病的诊断标志物。此外, 在肝性脑病高氨血症动物模型的脑组织中, *BDNF* 的蛋白和表达水平显著降低。<sup>36–40</sup> 而且, 当培养物暴露于氨时, 脑源性神经营养因子诱导的星形胶质细胞功能形态学变化被破坏。<sup>41</sup>

A



B

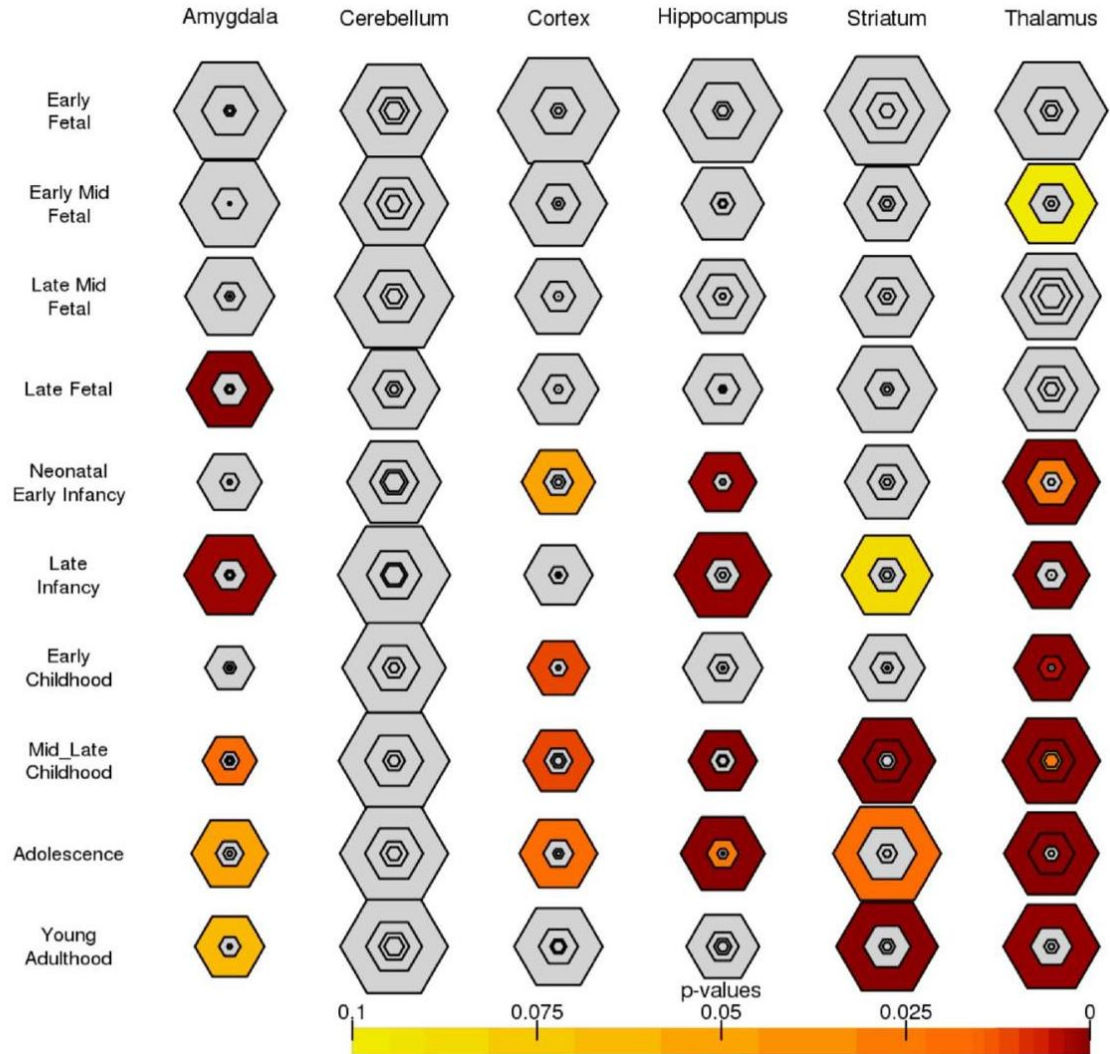


Figure 6. Tissue expression analysis for brain significant DEGs. (A) Brain region expression analysis of both upregulated and downregulated cerebral genes associated with HE. (B) Time-series-specific tissue expression analysis for demonstrating expression patterns of target genes using CSEA Web tool. The size of nodes indicated



pSI thresholds (values decrease from outside (0.05) to inside (0.0001)) and color-adjusted based on *P* value so that darker ones represent more significant brain regions during different periods. DEGs indicate differentially expressed genes; HE, hepatic encephalopathy.

图 6. 大脑显著差异表达基因的组织表达分析。(A) 与肝性脑病相关的大脑上调和下调基因的脑区表达分析。(B) 使用 CSEA 网络工具进行的时间序列特异性组织表达分析，以展示目标基因的表达模式。节点大小表示 pSI 阈值 (数值从外部 (0.05) 向内部 (0.0001) 减小)，颜色根据 *P* 值进行调整，颜色越深表示在不同时期的大脑区域越显著。DEGs 表示差异表达基因；HE 表示肝性脑病。

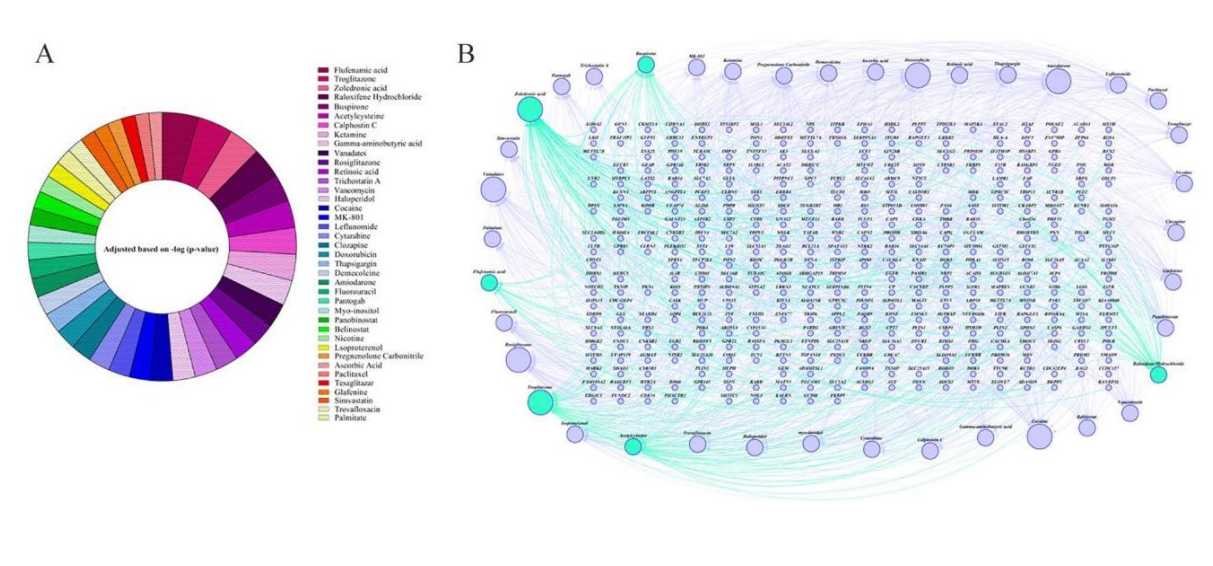


Figure 7. Drug/agent target prediction for main DEGs of cirrhosis-induced HE. (A) Thirty-nine significant drugs/agents were predicted for both cerebral upregulated and downregulated genes from DEGs in cirrhosis-induced HE using ToppGene database. All annotations are adjusted based on *P* value and presented as  $-\log(P \text{ value})$  in the colorful pie chart. The most significant agents are listed in the upper position of the right panel. (B) Drug-genetic network for DEGs associated with cirrhosis-induced HE. The network indicates the number of associated genes that predict each drug/agent. Green nodes have the lowest *P* value and greater nodes are more connected nodes (greater degree). DEGs indicate differentially expressed genes; HE, hepatic encephalopathy.

图 7. 肝硬化诱导的肝性脑病主要差异表达基因的药物/药剂靶点预测。(A) 使用 ToppGene 数据库，对肝硬化诱导的肝性脑病差异表达基因中大脑上调和下调的基因预测出 39 种显著的药物/药剂。所有注释均基于 *P* 值进行调整，并在彩色饼图中以  $-\log(P \text{ 值})$  表示。最显著的药剂列于右侧面板的上方。(B) 与肝硬化诱导的肝性脑病相关的差异表达基因的药物 - 基因网络。该网络表示预测每种药物/药剂的相关基因数量。绿色节点的 *P* 值最低，较大的节点表示连接更多的节点 (度数更大)。DEGs 表示差异表达基因；HE 表示肝性脑病。

The third hub gene ERBB2 (Erb-B2 receptor tyrosine kinase 2), named HER-2, HER-2/neu, and Erb-B2, is a member of the EGFR family of receptor tyrosine kinases, and due to the lack of ligand-binding domain, no ligands have yet been introduced for it. This protein strongly forms a heterodimer with other receptor family members such as Erb-B2 receptor tyrosine kinase 3 (ERBB3) and Erb-B2 receptor tyrosine kinase 4 (ERBB4) to facilitate ligand-binding process and its consequent activation of downstream signaling pathways.<sup>42</sup> These downstream signaling through MAPK, phosphoinositide 3-kinase (PI3K/Akt), protein kinase C (PKC), and finally signal transducer and activator of transcription (STAT) mediate cell proliferation and differentiation.<sup>42</sup> Activation of ERBB2 following brain injury triggers astrocyte proliferation and ensures the survival of neurons.<sup>43</sup> The mRNA and protein of

ERBB2 are abnormally increased in the liver tissues of patients with fulminant hepatitis and concanavalin A-induced fulminant hepatitis mouse model.<sup>44</sup> In a recent study, overexpression of cytoplasmic and nuclear ERBB2 and its downstream protein STAT3 was observed following immunohistochemistry analysis of 1125 liver samples from patients with different liver dysfunction.<sup>45</sup>

第三个枢纽基因 ERBB2(Erb-B2 受体酪氨酸激酶 2), 也被称为 HER - 2、HER - 2/neu 和 Erb - B2, 是受体酪氨酸激酶表皮生长因子受体 (EGFR) 家族的成员。由于缺乏配体结合域, 目前尚未发现与之结合的配体。该蛋白能与其他受体家族成员, 如 Erb - B2 受体酪氨酸激酶 3(ERBB3) 和 Erb - B2 受体酪氨酸激酶 4(ERBB4) 强烈形成异源二聚体, 以促进配体结合过程, 并随之激活下游信号通路。<sup>42</sup> 这些通过丝裂原活化蛋白激酶 (MAPK)、磷脂酰肌醇 3 - 激酶 (PI3K/Akt)、蛋白激酶 C (PKC), 最终通过信号转导和转录激活因子 (STAT) 的下游信号传导介导细胞增殖和分化。<sup>42</sup> 脑损伤后 ERBB2 的激活会触发星形胶质细胞增殖, 并确保神经元存活。<sup>43</sup> 在暴发性肝炎患者的肝组织和伴刀豆球蛋白 A 诱导的暴发性肝炎小鼠模型中, ERBB2 的信使核糖核酸 (mRNA) 和蛋白水平异常升高。<sup>44</sup> 最近一项研究中, 对 1125 份不同肝功能障碍患者的肝脏样本进行免疫组织化学分析后, 观察到细胞质和细胞核中的 ERBB2 及其下游蛋白 STAT3 过表达。<sup>45</sup>

The GFAP is another important hub gene in cirrhosis-induced HE genetic network. The GFAP proteins, monomeric intermediate filaments, are highly expressed in astrocytes to mediate dynamic properties of these cells for contributing the homeostasis of the CNS and maintaining the structure of the BBB.<sup>46</sup> Abnormal expression of cerebral *GFAP* (as an astrocyte reactivity marker) in many clinical, in vivo, and in vitro hyper-ammonemic studies has been examined previously. Postmortem examination of brain tissues from HE patients revealed a significant decrease in GFAP proteins in cerebral cortex and basal ganglia.<sup>47</sup> An increase in immunoreactivity of GFAP was also observed in postmortem cerebellum specimens from cirrhotic patients and nonalcoholic steatohepatitis.<sup>48,49</sup> Abnormal expression of *GFAP* was also reported in the brain sample after neurosurgery in a patient with HE.<sup>50</sup> In bile duct-ligated (BDL) rats as an animal model of HE, the expression of GFAP in substantia nigra, ventral tegmental area, hippocampus, and dorsal striatum decreased while in cerebral cortex strongly increased compared with control rats.<sup>39,51</sup> A decrease in the expression of GFAP in parahippocampal area of thioacetamide-induced HE animals was also obvious.<sup>52</sup> Furthermore, the expression of GFAP proteins in the brain tissue of swine models of HE was decreased and astroglial cells changed morphologically.<sup>53</sup> On the contrary, in other studies, GFAP immunoreactivity was significantly increased in hippocampal areas of thioacetamide-induced HE rats<sup>54,55</sup> and cerebral cortex of hyperammonemic rats,<sup>56</sup> whereas in BDL-induced cirrhosis and HE rats, opposite results were seen.<sup>55</sup> Ammonia on organotypic mice brain slice increased expression of GFAP and caused astrocyte swelling.<sup>57</sup> In vitro exposure of astrocyte cultures to ammonia significantly decreased the expression of GFAP filaments.

58

胶质纤维酸性蛋白 (GFAP) 是肝硬化诱发肝性脑病 (HE) 遗传网络中的另一个重要枢纽基因。GFAP 蛋白是单体中间丝, 在星形胶质细胞中高度表达, 调节这些细胞的动态特性, 有助于中枢神经系统 (CNS) 的稳态并维持血脑屏障 (BBB) 的结构。<sup>46</sup> 先前已在许多临床、体内和体外高氨血症研究中检测了脑内 *GFAP* (作为星形胶质细胞反应性标志物) 的异常表达。对肝性脑病患者脑组织的尸检显示, 大脑皮层和基底神经节中的 *GFAP* 蛋白显著减少。<sup>47</sup> 在肝硬化患者和非酒精性脂肪性肝炎患者的尸检小脑标本中, 也观察到 *GFAP* 免疫反应性增加。<sup>48,49</sup> 也有报道称, 一名肝性脑病患者神经手术后的脑样本中 *GFAP* 表达异常。<sup>50</sup> 在作为肝性脑病动物模型的胆管结扎 (BDL) 大鼠中, 与对照大鼠相比, 黑质、腹侧被盖区、海马和背侧纹状体中的 *GFAP* 表达降低, 而大脑皮层中的 *GFAP* 表达则显著增加。<sup>39,51</sup> 在硫代乙酰胺诱导的肝性脑病动物的海马旁区, *GFAP* 表达降低也很明显。<sup>52</sup> 此外, 肝性脑病猪模型脑组织中的 *GFAP* 蛋白表达降低, 星形胶质细胞形态发生改变。<sup>53</sup> 相反, 在其他研究中, 硫代乙酰胺诱导的肝性脑病大鼠的海马区<sup>54,55</sup> 和高氨血症大鼠的大脑皮层中, *GFAP* 免疫反应性显著增加,<sup>56</sup> 而在胆管结扎诱导的肝硬化和肝性脑病大鼠中, 则观察到相反的结果。<sup>55</sup> 氨作用于器官型小鼠脑切片会增加 *GFAP* 的表达, 并导致星形胶质细胞肿胀。<sup>57</sup> 在体外将星形胶质细胞培养物暴露于氨中, 会显著降低 *GFAP* 的表达。<sup>58</sup>

The fifth hub gene was *AQP4*, which is an integral membrane protein and main aquaporin water channel in the CNS and contributes to the brain water homeostasis. These channels mainly express and localize on astrocyte end-feet in place of the BBB and ensure normal water flow through the brain parenchyma.<sup>59</sup> The role of *AQP4* in the pathophysiology of HE and brain edema has been discussed previously.<sup>6</sup> Abnormal expression and mislocation of *AQP4* in the brain tissue following liver diseases may be responsible for the accumulation of neurotoxic substances in the brain interstitium and its consequences such as neuroinflammation, progression of astrocyte swelling and cerebral edema.<sup>6,60</sup> Postmortem analysis of brain samples from patients with liver failure has shown that the expression of mRNA and protein of *AQP4* significantly increased in perivascular astrocytes end-feet.<sup>61</sup> Increased expression of *AQP4* in the cerebral cortex, hippocampus, thalamus, and basal ganglia has been identified in acetaminophen-, thioacetamide- and BDL-induced liver failure and HE rodents.<sup>62–64</sup> Furthermore, *AQP4* depletion (knockout *AQP4*) in acetaminophen- and thioacetamide-induced HE mice significantly suppressed cerebral edema.<sup>65</sup> Some studies have reported that the expression of *AQP4* was not changed in the brain of galactosamine- and thioacetamide-induced HE and hyperammonemic rats, whereas it was significantly upregulated in BDL-induced cirrhosis rats.<sup>66–68</sup> Mislocation and reduced expression of *AQP4* water channels in the olfactory bulb and prefrontal cortex along with severe cognitive impairments were also observed in BDL-induced HE rats.<sup>60</sup> Hyperammonemic conditions in astrocyte cultures caused the mislocation of *AQP4* on the plasma membrane,<sup>69</sup> whereas in another study, it caused ammonia-induced upregulation of *AQP4* on the astrocyte membrane.<sup>70</sup>



第五个枢纽基因是 *AQP4*，它是一种整合膜蛋白，也是中枢神经系统 (CNS) 中的主要水通道蛋白水通道，有助于维持大脑的水平衡。这些通道主要在血脑屏障 (BBB) 处的星形胶质细胞终足上表达和定位，确保正常的水流经脑实质。<sup>59</sup> 此前已经讨论过 *AQP4* 在肝性脑病 (HE) 和脑水肿病理生理学中的作用。<sup>6</sup> 肝脏疾病后脑组织中 *AQP4* 的异常表达和错位可能导致神经毒性物质在脑间质中积聚，进而引发神经炎症、星形胶质细胞肿胀加剧和脑水肿等后果。<sup>6,60</sup> 对肝衰竭患者脑样本的尸检分析表明，血管周围星形胶质细胞终足中 *AQP4* 的 mRNA 和蛋白质表达显著增加。<sup>61</sup> 在对乙酰氨基酚、硫代乙酰胺和胆管结扎 (BDL) 诱导的肝衰竭和肝性脑病啮齿动物模型中，已发现大脑皮层、海马体、丘脑和基底神经节中 *AQP4* 的表达增加。<sup>62-64</sup> 此外，在对乙酰氨基酚和硫代乙酰胺诱导的肝性脑病小鼠中，敲除 *AQP4* (敲除 *AQP4*) 可显著抑制脑水肿。<sup>65</sup> 一些研究报告称，在半乳糖胺和硫代乙酰胺诱导的肝性脑病和高氨血症大鼠的大脑中，*AQP4* 的表达没有变化，而在胆管结扎诱导的肝硬化大鼠中，其表达显著上调。<sup>66-68</sup> 在胆管结扎诱导的肝性脑病大鼠中，还观察到嗅球和前额叶皮质中 *AQP4* 水通道的错位和表达降低，同时伴有严重的认知障碍。<sup>60</sup> 星形胶质细胞培养中的高氨血症条件会导致 *AQP4* 在质膜上的错位，<sup>69</sup> 而另一项研究则表明，它会导致氨诱导的星形胶质细胞膜上 *AQP4* 表达上调。<sup>70</sup>

Table 2. Predicted transcription factors and miRNAs for genes associated with cirrhosis-induced HE.

表 2. 肝硬化诱导的肝性脑病相关基因的预测转录因子和微小 RNA。

INDEX	NAME	PVALUE	-LOG (P VALUE)
Enriched TFs for upregulated genes			
1.	SMAD4	.00003208	4.49376564
2.	NR5A2	.0001679	3.774949304
3.	NFIA	.000246	3.609064893
4.	UBTF	.001286	2.890759031
5.	HNF1A	.0027	2.568636236
6.	MXI1	.003579	2.446238302
7.	MAPK14	.007077	2.150150804
Predicted miRNAs for upregulated genes			
1.	hsa-miR-325-3p	2.16E-15	14.66535
2.	hsa-miR-124-3p.1	6.32E-13	12.19915
3.	hsa-miR-495-3p	4.35E-08	7.36181
4.	hsa-miR-24-3p	9.16E-08	7.037915
5.	hsa-miR-133a-3p.1	6.55E-07	6.184024
6.	hsa-miR-506-3p	6.98E-07	6.156145
7.	hsa-miR-124-3p.2	6.98E-07	6.156145
8.	hsa-miR-497-5p	9.20E-07	6.036401
9.	hsa-miR-16-5p	9.20E-07	6.036401
10.	hsa-miR-15a-5p	9.20E-07	6.036401
Enriched TFs for downregulated genes			
1.	TCF4	.004196	2.37716452
2.	TEAD2	.004676	2.330125498
3.	HNF1A	.01059	1.97510404
4.	MEF2A	.01267	1.897223385
5.	JUN	.0192	1.716698771
6.	NFIC	.02462	1.608711951
7.	SRF	.02512	1.599980365
Predicted miRNAs for downregulated genes			
1.	hsa-miR-27b-3p	1.51E-12	11.81987412
2.	hsa-miR-27a-3p	1.51E-12	11.81987412
3.	hsa-miR-23a-3p	1.11E-10	9.953895213
4.	hsa-miR-23b-3p	1.11E-10	9.953895213
5.	hsa-miR-23c	1.11E-10	9.953895213
6.	hsa-miR-124-3p.1	1.20E-10	9.920818754
7.	hsa-miR-30e-5p	5.78E-10	9.238072162
8.	hsa-miR-30a-5p	5.78E-10	9.238072162
9.	hsa-miR-30d-5p	5.78E-10	9.238072162
10.	hsa-miR-30b-5p	5.78E-10	9.238072162

索引	名称	P 值	-对数 (P 值)
上调基因的富集转录因子 (TFs)			
1.	SMAD4(SMAD4 蛋白)	.00003208	4.49376564
2.	NR5A2(核受体亚家族 5A 成员 2)	.0001679	3.774949304
3.	NFIA(核因子 I - A)	.000246	3.609064893
4.	UBTF(上游结合转录因子)	.001286	2.890759031
5.	HNF1A(肝细胞核因子 1 $\alpha$ )	.0027	2.568636236
6.	MXI1(MAX 相互作用蛋白 1)	.003579	2.446238302
7.	MAPK14(丝裂原活化蛋白激酶 14)	.007077	2.150150804
上调基因的预测微小 RNA(miRNAs)			
1.	hsa - miR - 325 - 3p(人微小 RNA - 325 - 3p)	2.16E-15	14.66535
2.	hsa - miR - 124 - 3p.1(人微小 RNA - 124 - 3p.1)	6.32E-13	12.19915
3.	hsa - miR - 495 - 3p(人微小 RNA - 495 - 3p)	4.35E-08	7.36181
4.	hsa - miR - 24 - 3p(人微小 RNA - 24 - 3p)	9.16E-08	7.037915
5.	hsa - miR - 133a - 3p.1(人微小 RNA - 133a - 3p.1)	6.55E-07	6.184024
6.	hsa - miR - 506 - 3p(人微小 RNA - 506 - 3p)	6.98E-07	6.156145
7.	hsa - miR - 124 - 3p.2(人微小 RNA - 124 - 3p.2)	6.98E-07	6.156145
8.	hsa - miR - 497 - 5p(人微小 RNA - 497 - 5p)	9.20E-07	6.036401
9.	hsa - miR - 16 - 5p(人微小 RNA - 16 - 5p)	9.20E-07	6.036401
10.	hsa - miR - 15a - 5p(人微小 RNA - 15a - 5p)	9.20E-07	6.036401
下调基因的富集转录因子 (TFs)			
1.	TCF4(转录因子 4)	.004196	2.37716452
2.	TEAD2(TEA 结构域转录因子 2)	.004676	2.330125498
3.	HNF1A(肝细胞核因子 1 $\alpha$ )	.01059	1.97510404
4.	MEF2A(肌细胞增强因子 2A)	.01267	1.897223385
5.	JUN(原癌基因蛋白 JUN)	.0192	1.716698771
6.	NFIC(核因子 I - C)	.02462	1.608711951
7.	SRF(血清反应因子)	.02512	1.599980365
下调基因的预测微小 RNA(miRNAs)			
1.	hsa - miR - 27b - 3p(人微小 RNA - 27b - 3p)	1.51E-12	11.81987412
2.	hsa - miR - 27a - 3p(人微小 RNA - 27a - 3p)	1.51E-12	11.81987412
3.	hsa - miR - 23a - 3p(人微小 RNA - 23a - 3p)	1.11E-10	9.953895213
4.	hsa - miR - 23b - 3p(人微小 RNA - 23b - 3p)	1.11E-10	9.953895213
5.	hsa - miR - 23c(人微小 RNA - 23c)	1.11E-10	9.953895213
6.	hsa - miR - 124 - 3p.1(人微小 RNA - 124 - 3p.1)	1.20E-10	9.920818754
7.	hsa - miR - 30e - 5p(人微小 RNA - 30e - 5p)	5.78E-10	9.238072162
8.	hsa - miR - 30a - 5p(人微小 RNA - 30a - 5p)	5.78E-10	9.238072162
9.	hsa - miR - 30d - 5p(人微小 RNA - 30d - 5p)	5.78E-10	9.238072162
10.	hsa - miR - 30b - 5p(人微小 RNA - 30b - 5p)	5.78E-10	9.238072162

HNF1A, hepatocyte nuclear factor 1-alpha; JUN, AP-1 transcription factor subunit; MAPK14, p38 mitogen-activated protein kinase; MEF2A, myocyte enhancer factor 2A; MXI1, MAX interactor 1, dimerization protein; NFIA, nuclear factor I A; NFIC, nuclear factor I C; NR5A2, nuclear receptor subfamily 5 group a member 2; SMAD4, SMAD family member 4, mothers against decapentaplegic homolog 4; SRF, serum response factor; TCF4,

transcription factor 4; TEAD2, TEA domain transcription factor 2; UBTF, upstream binding transcription factor.

HNF1A, 肝细胞核因子 1- $\alpha$ (hepatocyte nuclear factor 1-alpha); JUN, 激活蛋白-1 转录因子亚基 (AP-1 transcription factor subunit); MAPK14, p38 丝裂原活化蛋白激酶 (p38 mitogen-activated protein kinase); MEF2A, 肌细胞增强因子 2A(myocyte enhancer factor 2A); MXI1, MAX 相互作用蛋白 1(MAX interactor 1), 二聚化蛋白; NFIA, 核因子 I A(nuclear factor I A); NFIC, 核因子 I C(nuclear factor I C); NR5A2, 核受体亚家族 5 A 组成员 2(nuclear receptor subfamily 5 group a member 2); SMAD4, SMAD 家族成员 4(SMAD family member 4), 抗果蝇畸形同源物 4(mothers against decapentaplegic homolog 4); SRF, 血清反应因子 (serum response factor); TCF4, 转录因子 4(transcription factor 4); TEAD2, TEA 结构域转录因子 2(TEA domain transcription factor 2); UBTF, 上游结合转录因子 (upstream binding transcription factor)。

The SLC1A2 known as excitatory amino acid transporter 2 (EAAT2) and glutamate transporter 1 (GLT-1) is a solute carrier family that is mainly expressed in astroglial cells which mediates the reuptake of the glutamate neurotransmitters from excitatory synaptic spaces in the CNS that guarantee normal neuronal functions.<sup>71</sup> Studies on animal models of HE and hyperammonemic condition indicated that the protein expression of EAAT2 significantly decreased in the brain which led to an increase in the concentration of extracellular glutamate and progression of cerebral edema.<sup>72–76</sup>

溶质载体家族 1 成员 2(SLC1A2), 也被称为兴奋性氨基酸转运体 2(excitatory amino acid transporter 2, EAAT2) 和谷氨酸转运体 1(glutamate transporter 1, GLT-1), 主要在星形胶质细胞中表达, 它介导中枢神经系统 (CNS) 中兴奋性突触间隙谷氨酸神经递质的再摄取, 以保证神经元的正常功能。<sup>71</sup> 对肝性脑病 (HE) 动物模型和高氨血症状态的研究表明, 大脑中 EAAT2 的蛋白表达显著降低, 导致细胞外谷氨酸浓度增加和脑水肿进展。<sup>72–76</sup>

Pathway analysis revealed fatty acid beta-oxidation and serotonin receptor 2 and ELK-SRF/GATA4 signaling were 2 important involved pathways for upregulated and downregulated cerebral DEGs, respectively. Fatty acid beta-oxidation is a process by which fatty acids break down to acetyl coenzyme A (acetyl CoA) to produce adenosine triphosphate (ATP) in mitochondria through the tricarboxylic acid cycle. It has long been believed that glucose was the main fuel source for neural cells that were maintained during the oxidative phosphorylation in neurons and glycolysis in astrocytes. In the brain, fatty acids can transport across the BBB via fatty acid transporters or passive diffusion.<sup>77,78</sup> However, recent evidence suggests that the oxidation of fatty acids in the astrocyte's mitochondria is another significant source of energy in the CNS.<sup>79–82</sup> Recent studies have also revealed that genes associated with fatty acid oxidation are more expressed in astrocytes compared with neurons.<sup>81,83</sup> Carnitine palmitoyltransferase 1a (CPT1a) is the main protein responsible for the production of acyl-carnitine from acyl CoA in the outer membrane of mitochondria, a process that is important in fatty acid beta-oxidation<sup>84</sup> and mainly expressed on astroglial cells into the CNS<sup>85</sup> but not on neurons. Glutamate toxicity, mitochondrial damage, depletion of cellular ATP stores, and decreased energy metabolism have been reported in the brain of animal models of HE<sup>86,87</sup> as well as ammonia-exposed astrocyte cultures.<sup>88–91</sup> Exposure of the primary culture of astrocytes to glutamate inhibits fatty acid beta-oxidation.<sup>81</sup> Glutamate toxicity and mitochondrial impairments may be responsible for ATP depletion and decreased brain energy metabolisms following HE due to the inhibition of astroglial fatty acid oxidation.

通路分析显示, 脂肪酸  $\beta$ -氧化以及血清素受体 2 和 ELK - SRF/GATA4 信号通路分别是上调和下调的大脑差异表达基因 (DEGs) 所涉及的两条重要通路。脂肪酸  $\beta$ -氧化是脂肪酸分解为乙酰辅酶 A (乙酰 CoA) 的过程, 通过三羧酸循环在线粒体中产生三磷酸腺苷 (ATP)。长期以来, 人们认为葡萄糖是神经细胞的主要能量来源, 在神经元的氧化磷酸化和星形胶质细胞的糖酵解过程中维持神经细胞的功能。在大脑中, 脂肪酸可以通过脂肪酸转运蛋白或被动扩散穿过血脑屏障 (BBB)。<sup>77,78</sup> 然而, 最近的证据表明, 星形胶质细胞线粒体中脂肪酸的氧化是中枢神经系统中另一个重要的能量来源。<sup>79-82</sup> 最近的研究还表明, 与神经元相比, 星形胶质细胞中与脂肪酸氧化相关的基因表达更多。<sup>81,83</sup> 肉碱棕榈酰转移酶 1a (Carnitine palmitoyltransferase 1a, CPT1a) 是负责在线粒体外膜将酰基辅酶 A 转化为酰基肉碱的主要蛋白质, 这一过程在脂肪酸  $\beta$ -氧化中很重要<sup>84</sup>, 并且主要在中枢神经系统的星形胶质细胞中表达<sup>85</sup>, 而不在神经元中表达。在 HE<sup>86,87</sup> 动物模型的大脑以及暴露于氨的星形胶质细胞培养物中, 均有谷氨酸毒性、线粒体损伤、细胞 ATP 储存耗竭和能量代谢降低的报道。<sup>88-91</sup> 原代培养的星形胶质细胞暴露于谷氨酸会抑制脂肪酸  $\beta$ -氧化。<sup>81</sup> 由于星形胶质细胞脂肪酸氧化受到抑制, 谷氨酸毒性和线粒体损伤可能是肝性脑病后 ATP 耗竭和大脑能量代谢降低的原因。

The dysfunctional serotonergic system has been reported in HE that is implicated in the onset of neuropsychiatric manifestations and behavior changes of HE.<sup>92</sup> Increased serotonergic tone and a raise in extracellular brain serotonin as an inhibitory neurotransmitter have been revealed in animal models of HE.<sup>93</sup> Furthermore, an increase in binding sites for serotonin receptor 2 has been shown in the hippocampus of cirrhosis-induced HE patients.<sup>94</sup> Also, the brain concentration of serotonin was correlated with the degree of shunting and the level of blood ammonia in portal-systemic shunting rats.<sup>95</sup>

已有报道称, 肝性脑病 (HE) 中存在血清素能系统功能障碍, 这与肝性脑病神经精神症状的发作和行为改变有关。<sup>92</sup> 在肝性脑病动物模型中, 已发现血清素能张力增加, 作为抑制性神经递质的细胞外脑血清素水平升高。<sup>93</sup> 此外, 在肝硬化诱发的肝性脑病患者的海马体中, 血清素受体 2 的结合位点增加。<sup>94</sup> 而且, 在门体分流大鼠中, 大脑血清素浓度与分流程度和血氨水平相关。<sup>95</sup>

Here, we suggest astrocytes, Bergmann glia, oligodendrocytes, and satellite glial cells as the mainly affected cellular types in association with upregulated cerebral DEGs, whereas photoreceptor cells, pyramidal cells, and retinal ganglion cells were the mainly involved cell types in relation to downregulation DEGs (Figure 5). Therefore, in our bioinformatic analyses, upregulated genes are mostly implicated in the brain glial cells and downregulated genes are mentioned in the involvement of main visual cells and neurons which can be well investigated by future experimental studies.

在此, 我们认为星形胶质细胞、伯格曼胶质细胞、少突胶质细胞和卫星胶质细胞是与上调的大脑差异表达基因相关的主要受影响细胞类型, 而光感受器细胞、锥体细胞和视网膜神经节细胞是与下调的差异表达基因相关的主要涉及细胞类型 (图 5)。因此, 在我们的生物信息学分析中, 上调的基因大多与大脑胶质细胞有关, 下调的基因与主要视觉细胞和神经元的参与有关, 这些可以通过未来的实验研究进行深入探究。

The result of tissue expression analysis indicated that thalamus, striatum, hippocampus, cortex, and amygdala were more important brain regions that were affected by cirrhosis and HE (Figure 6A). Surprisingly, time-series tissue expression analyses showed that thalamus can be considered an exclusive brain region in cirrhotic patients with different age groups (Figure 6B). The striatum, hippocampus, and cerebral cortex may be more involved in adolescent patients with HE (Figure 6B).

组织表达分析结果表明, 丘脑、纹状体、海马体、皮质和杏仁核是受肝硬化和肝性脑病 (HE) 影响较大的脑区 (图 6A)。令人惊讶的是, 时间序列组织表达分析显示, 丘脑可被视为不同年龄组肝硬化患者特有的脑区 (图 6B)。纹状体、海马体 and 大脑皮质可能更多地参与青少年肝性脑病患者的病情 (图 6B)。

As gene expression patterns can be strongly regulated at posttranscriptional levels, we also predicted 14 TFs and 20 miRNAs, which can target some DEGs from cirrhosis patients (Table 2). The miRNAs can mediate many cellular processes such as proliferation, migration, differentiation, and apoptosis through downregulation of their target mRNA and with dys-regulation of specific mRNA may develop diseases.<sup>96</sup> Targeting these miRNAs as a gene-regulatory option can be considered a probable therapeutic target for cirrhosis-induced HE in future studies.

由于基因表达模式在转录后水平可受到强烈调控, 我们还预测了 14 种转录因子 (TFs) 和 20 种微小 RNA(miRNAs), 它们可以靶向肝硬化患者的一些差异表达基因 (DEGs)(表 2)。miRNAs 可通过下调其靶 mRNA 来介导许多细胞过程, 如增殖、迁移、分化和凋亡, 特定 mRNA 的失调可能会引发疾病。<sup>96</sup> 在未来的研究中, 将这些 miRNAs 作为基因调控的靶点, 可被视为肝硬化所致肝性脑病的一种潜在治疗靶点。

Finally, our study predicted 39 significant and potentially effective drugs/agents for HE (Figure 7). Among these agents, flufenamic acid (a cyclooxygenase inhibitor), troglitazone (a peroxisome proliferator-activated receptors (PPARs) activator), and glafenine have anti-inflammatory effects. As inflammation along with hyperammonemia can exacerbate manifestations of HE, prescription of anti-inflammatory drugs may be effective.<sup>97,98</sup> Trichostatin A (antifungal), vancomycin (against gram-positive bacteria), and trovafloxacin (as a broad-spectrum antibiotic) were also annotated as antibiotic agents. Antibiotic therapy along with non-absorbable disaccharides considered a first-line therapeutic option for the management of HE.<sup>99</sup> Effective therapy with vancomycin was suggested for patients with HE.<sup>100–102</sup> Other important predicted medication therapies for HE are dietary supplements and antioxidant agents such as acetylcysteine (also known as N-acetylcysteine), retinoic acid (known as all-trans-retinol), and ascorbic acid. N-acetylcysteine therapy significantly improved the survival of patients with paracetamol-induced acute liver failure and non-paracetamol-associated liver failure and HE.<sup>103,104</sup> Antipsychotic drugs such as haloperidol (as a dopamine D2 receptor antagonist) and clozapine (an antagonist at the 5-HT<sub>2A</sub> subunit of the serotonin receptor) were also associated with HE in our study. Administration of haloperidol sufficiently controls delirium, agitation, and epileptic seizures in patients with HE.<sup>105</sup> The protective effect of clozapine on HE is still debated. Previous studies have reported hepatotoxic effects for clozapine.<sup>106,107</sup> A number of antineoplastic agents such as calphostin C (a potent inhibitor of protein kinase C), cytarabine, doxorubicin, demecolcine (as a microtubule-depolymerizing agent), fluorouracil (as a thymidylate synthase inhibitor), panobinostat (as a non-selective histone deacetylase inhibitor), belinostat (as a histone deacetylase inhibitor), and paclitaxel were also predicted. Furthermore, amiodarone (an antiarrhythmic agent) and isoproterenol (a non-selective  $\beta$  adrenoceptor agonist) were other annotated drugs for cirrhosis-induced HE. Rosiglitazone (as a peroxisome proliferator-activated receptors activator), tesaglitazar, and myo-inositol (a natural insulin sensitizer) as antidiabetic agents were also suggested for HE. Rosiglitazone therapy significantly decreased the risk of cirrhosis in patients with type 2 diabetes and improved the hepatic metabolism of asymmetric dimethylarginine in rat models of HE.<sup>108,109</sup> Buspirone as an agonist of the serotonin 5-HT<sub>1A</sub> receptor was also predicted in the study. The protective effect of buspirone in carbon tetrachloride-induced cirrhosis through an antioxidant-dependent manner has been confirmed.<sup>110</sup>

最后, 我们的研究预测了 39 种对肝性脑病有显著且潜在疗效的药物/药剂 (图 7)。在这些药剂中, 氟芬那酸 (一种环氧化酶抑制剂)、曲格列酮 (一种过氧化物酶体增殖物激活受体 (PPARs) 激活剂) 和格拉非宁具有抗炎作用。由于炎症和高氨血症会加重肝性脑病的症状, 开具抗炎药物可能会有效果。<sup>97,98</sup> 曲古抑菌素 A (抗真菌药)、万古霉素 (抗革兰氏阳性菌) 和曲伐沙星 (广谱抗生素) 也被标注为抗生素类药剂。抗生素治疗联合不可吸收的二糖被认为是治疗肝性脑病的一线治疗方案。<sup>99</sup> 有研究建议对肝性脑病患者采用万古霉素进行有效治疗。<sup>100–102</sup> 其他重要的预测用于治疗肝性脑病的药物疗法包括膳食补充剂和抗氧化剂, 如乙酰半胱氨酸 (也称为 N - 乙酰半胱氨酸)、视黄酸 (也称为全反式视黄醇) 和抗坏血酸。N - 乙酰半胱氨酸治疗显著提高了对乙酰氨基酚所致急性肝衰竭、非对乙酰氨基酚相关肝衰竭和肝性脑病患者的生存率。<sup>103,104</sup> 在我们的研究中, 抗精神病药物如氟哌啶醇 (多巴胺 D2 受体拮抗剂) 和氯氮平 (血清素受体 5 - HT<sub>2A</sub> 亚基的拮抗剂) 也与肝性脑病有关。给予氟哌啶醇可有效控制肝性脑病患者的谵妄、躁动和癫痫发作。<sup>105</sup> 氯氮平对肝性脑病的保护作用仍存在争议。先前的研究报道了氯氮平的肝毒性作用。<sup>106,107</sup> 还预测了一些抗肿瘤药物, 如钙磷霉素 C (一种强效的蛋白激酶 C 抑制剂)、阿糖胞苷、阿霉素、秋水仙胺 (一种微管解聚剂)、氟尿嘧啶 (胸苷酸合成酶抑制剂)、帕比司他 (一种非选择性组蛋白去乙酰化酶抑制剂)、贝利司他 (组蛋白去乙酰化酶抑制剂) 和紫杉醇。此外, 胺碘酮 (抗心律失常药) 和异丙肾上腺素 (非选择性  $\beta$  肾上腺素能受体激动剂) 也是标注用于肝硬化所致肝性脑病的药物。罗格列酮 (过氧化物酶体增殖物激活受体激活剂)、替扎吉坦和肌醇 (一种天然胰岛素增敏剂) 等抗糖尿病药物也被建议用于治疗肝性脑病。罗格列酮治疗显著降低了 2 型糖尿病患者患肝硬化的风险, 并改善了肝性脑病大鼠模型中不对称二甲精氨酸的肝脏代谢。<sup>108,109</sup> 本研究还预测了丁螺环酮 (血清素 5 - HT<sub>1A</sub> 受体激动剂)。丁螺环酮通过抗氧化依赖方式对四氯化碳诱导的肝硬化的保护作用已得到证实。<sup>110</sup>

## Conclusion

### 结论

Altogether, we comprehensively analyzed DEGs from cerebral tissues of cirrhotic patients with HE compared with healthy subjects through an integrated bioinformatics approach. We then proceeded our analysis through different public databases such as Enricher, ToppGene, and CSEA to reveal the mainly involved biological processes, signaling pathways, and brain regions as well as identify potential effective drugs for HE. These findings not only confirmed many previously known involved signaling pathways but also disclosed new insights into other molecular and cellular mechanisms of HE. Furthermore, our results identified some hub genes from significant DEGs in relation to HE that may provide new therapeutic targets for HE. The small sample size can be considered the main limitation of the study and collecting more clinical samples from HE patients can make the study results more reliable. Moreover, the findings should be studied more thoroughly by in vivo and in vitro experiments in the future.

总的来说，我们通过综合生物信息学方法，全面分析了肝性脑病 (HE) 肝硬化患者与健康受试者脑组织中的差异表达基因 (DEGs)。然后，我们通过 Enricher、ToppGene 和 CSEA 等不同的公共数据库进行分析，以揭示主要涉及的生物过程、信号通路和脑区，并确定可能对肝性脑病有效的药物。这些发现不仅证实了许多先前已知的相关信号通路，还揭示了肝性脑病其他分子和细胞机制的新见解。此外，我们的研究结果从与肝性脑病相关的显著差异表达基因中确定了一些关键基因，这些基因可能为肝性脑病提供新的治疗靶点。样本量小可被视为本研究的主要局限性，收集更多肝性脑病患者的临床样本可使研究结果更可靠。此外，未来应通过体内和体外实验对这些发现进行更深入的研究。

## Author Contributions

### 作者贡献

A Sepehrinezhad designed the study, carried out the literature review and data analysis, drew the illustrations, and drafted the manuscript. A Shahbazi designed the study, supervised the work, and participated in drafting the manuscript. FSL drafted the manuscript, critically revised, and scientifically edited the manuscript. SSN also scientifically and grammatically rechecked the revised manuscript. All authors read and approved the final manuscript.

A Sepehrinezhad 设计了研究，进行了文献综述和数据分析，绘制了插图，并起草了手稿。A Shahbazi 设计了研究，监督了工作，并参与了手稿的起草。FSL 起草了手稿，进行了严格修订和科学编辑。SSN 也对修订后的手稿进行了科学和语法上的复查。所有作者都阅读并批准了最终手稿。

## Ethics approval and consent to participate Not applicable.

### 伦理批准和参与同意不适用。

## Consent for publication

### 发表同意

Not applicable.

不适用。

## Data Availability Statement

### 数据可用性声明

All data generated or analyzed during this study are included in this published article and its supplementary information file.



本研究期间生成或分析的所有数据均包含在这篇已发表的文章及其补充信息文件中。

## Supplemental Material

### 补充材料

Supplemental material for this article is available online.

本文的补充材料可在线获取。

## REFERENCES

### 参考文献

1. Bustamante J, Rimola A, Ventura PJ, et al. Prognostic significance of hepatic encephalopathy in patients with cirrhosis. *J Hepatol.* 1999;30:890-895. doi:10.1016/s0168-8278(99)80144-5.
2. Martín-Valenzuela S, Borrás-Barrachina A, Gallego J-J, et al. Motor and cognitive performance in patients with liver cirrhosis with minimal hepatic encephalopathy. *J Clin Med.* 2020;9:2154.
3. Romero-Gómez M, Montagnese S, Jalan R. Hepatic encephalopathy in patients with acute decompensation of cirrhosis and acute-on-chronic liver failure. *J Hepatol.* 215;62:437-447. doi:10.1016/j.jhep.2014.09.005.
4. Sharma BC, Sharma P, Agrawal A, Sarin SK. Secondary prophylaxis of hepatic encephalopathy: an open-label randomized controlled trial of lactulose versus placebo. *Gastroenterology.* 2009;137:885-891, 891.e881. doi:10.1053/j.gastro.2009.05.056.
5. Jayakumar AR, Rama Rao KV, Norenberg MD. Neuroinflammation in hepatic encephalopathy: mechanistic aspects. *J Clin Exp Hepatol.* 2015;5:S21- S28. doi:10.1016/j.jceh.2014.07.006.
6. Sepehrinezhad A, Zarifkar A, Namvar G, Shahbazi A, Williams R. Astrocyte swelling in hepatic encephalopathy: molecular perspective of cytotoxic edema. *Metab Brain Dis.* 2020;35:559-578. doi:10.1007/s11011-020-00549-8.
7. Montagnese S, Russo FP, Amodio P, et al. Hepatic encephalopathy 2018: a clinical practice guideline by the Italian Association for the Study of the Liver (AISF). *Dig Liver Dis.* 2019;51:190-205. doi:10.1016/j.dld.2018.11.035.
8. Campagna F, Montagnese S, Schiff S, et al. Cognitive impairment and electroencephalographic alterations before and after liver transplantation: what is reversible? *Liver Transpl.* 2014;20:977-986. doi:10.1002/lt.23909.
9. Wang Z, Lachmann A, Ma'ayan A. Mining data and metadata from the Gene Expression Omnibus. *Biophys Rev.* 2019;11:103-110. doi:10.1007/s12551-018-0490-8.
10. Manoochehri H, Jalali A, Tanzadehpanah H, Taherkhani A, Saidijam M. Identification of key gene targets for sensitizing colorectal cancer to chemoradiotherapy: an integrative network analysis on multiple transcriptomics data. *J Gastrointest Cancer.* 2022;53:649-668. doi:10.1007/s12029-021-00690-2.
11. Taz TA, Ahmed K, Paul BK, et al. Network-based identification genetic effect of SARS-CoV-2 infections to Idiopathic pulmonary fibrosis (IPF) patients. *Brief Bioinform.* 2021;22:1254-1266. doi:10.1093/bib/bbaa235.

12. Szklarczyk D, Gable AL, Nastou KC, et al. The STRING database in 2021: customizable protein-protein networks, and functional characterization of user-uploaded gene/measurement sets. *Nucleic Acids Res.* 2021;49:D605-D612.
13. Sepehrinezhad A, Shahbazi A, Bozorgmehr A, et al. STAT3 and NTRK2 genes predicted by the bioinformatics approach may play important roles in the pathogenesis of multiple sclerosis and obsessive-compulsive disorder. *J Pers Med.* 2022;12:1043. doi:10.3390/jpm12071043.
14. Wu L, Chen Y, Wan L, et al. Identification of unique transcriptomic signatures and key genes through RNA sequencing and integrated WGCNA and PPI network analysis in HIV infected lung cancer. *Cancer Med.* 2022;12:949- 960. doi:10.1002/cam4.4853.
15. Moazeny M, Salari A, Hojati Z, Esmaeili F. Comparative analysis of protein-protein interaction networks in neural differentiation mechanisms. *Differentiation.* 2022;126:1-9. doi:10.1016/j.diff.2022.05.003.
16. Sepehrinezhad A, Rezaeitalab F, Shahbazi A, Sahab-Negah S. A computational-based drug repurposing method targeting SARS-CoV-2 and its neurological manifestations genes and signaling pathways. *Bioinform Biol Insights.* 2021;15:11779322211026728.
17. Božić D, Baralić K, Zivančević K, Djukić-Cosić D. Toxic potential of combined sulforaphane/Pseudomonas aeruginosa mannose sensitive hemagglutinin treatment in cancer patients. *Arch Pharm.* 2022;72:S607-S608.
18. Martinou EG, Moller-Levet CS, Angelidi AM. PBX4 functions as a potential novel oncopromoter in colorectal cancer: a comprehensive analysis of the PBX gene family. *Am J Cancer Res.* 2022;12:585-600.
19. Barneh F, Mirzaie M, Nickchi P, et al. Integrated use of bioinformatic resources reveals that co-targeting of histone deacetylases, IKBK and SRC inhibits epithelial-mesenchymal transition in cancer. *Brief Bioinform.* 2019;20:717-731. doi:10.1093/bib/bby030.
20. Zhang F, Xia M, Jiang J, et al. Machine learning and bioinformatics to identify 8 autophagy-related biomarkers and construct gene regulatory networks in dilated cardiomyopathy. *Sci Rep.* 2022;12:15030. doi:10.1038/s41598-022-19027-5.
21. Dai Y, Hu R, Liu A, et al. WebCSEA: web-based cell-type-specific enrichment analysis of genes [published online ahead of print May 24, 2022]. *Nucleic Acids Res.* doi:10.1093/nar/gkac392.
22. Hadjihambi A, Arias N, Sheikh M, Jalan R. Hepatic encephalopathy: a critical current review. *Hepatol Int.* 2018;12:135-147. doi:10.1007/s12072-017-9812-3.
23. Wee P, Wang Z. Epidermal growth factor receptor cell proliferation signaling pathways. *Cancers (Basel).* 2017;9:52. doi:10.3390/cancers9050052.
24. Kömüves LG, Feren A, Jones AL, Fodor E. Expression of epidermal growth factor and its receptor in cirrhotic liver disease. *J Histochem Cytochem.* 2000;48:821-830. doi:10.1177/002215540004800610.
25. Fuchs BC, Hoshida Y, Fujii T, et al. Epidermal growth factor receptor inhibition attenuates liver fibrosis and development of hepatocellular carcinoma. *Hepatology.* 2014;59:1577-1590. doi:10.1002/hep.26898.
26. Bhushan B, Chavan H, Borude P, et al. Dual role of epidermal growth factor receptor in liver injury and regeneration after acetaminophen overdose in mice. *Toxicol Sci.* 2017;155:363-378. doi:10.1093/toxsci/kfw213.
27. Choung S, Kim JM, Joung KH, Lee ES, Kim HJ, Ku BJ. Epidermal growth factor receptor inhibition attenuates non-alcoholic fatty liver disease in diet-induced obese mice. *Plos One.* 2019;14:e0210828. doi:10.1371/journal.pone.0210828.
28. Tanabe KK, Lemoine A, Finkelstein DM, et al. Epidermal growth factor gene functional polymorphism and the risk of hepatocellular carcinoma in patients with cirrhosis. *JAMA.* 2008;299:53-60. doi:10.1001/jama.2007.65.
29. KohlaMAS, Al-HaddadOK, NadaA, et al. Association of serum levels of epidermal growth factor with disease severity in patients with unresectable hepatocellular carcinoma. *Hepatoma Res.* 2016;2:18-25. doi:10.4103/2394-5079.168959.

30. Dai H, Jia G, Wang W, et al. Genistein inhibited ammonia induced astrocyte swelling by inhibiting NF- $\kappa$ B activation-mediated nitric oxide formation. *Metab Brain Dis*. 2017;32:841-848.

31. Chen F, Hori T, Ohashi N, Baine AM, Eckman CB, Nguyen JH. Occludin is regulated by epidermal growth factor receptor activation in brain endothelial cells and brains of mice with acute liver failure. *Hepatology*. 2011;53:1294- 1305. doi:10.1002/hep.24161.

急性肝衰竭小鼠的细胞和大脑。《肝脏病学》。2011 年；53 卷:1294 - 1305 页。doi:10.1002/hep.24161。

32. Miranda M, Morici JF, Zanoni MB, Bekinschtein P. Brain-derived neurotrophic factor: a key molecule for memory in the healthy and the pathological brain. *Front Cell Neurosci*. 2019;13:363. doi:10.3389/fncel.2019.00363.

33. Wilasco MI, Uribe-Cruz C, Santetti D, Pfaffenseller B, Dornelles CT, da Sil-veira TR. Brain-derived neurotrophic factor in children and adolescents with cirrhosis due to biliary atresia. *Ann Nutr Metab*. 2016;69:1-8. doi:10.1159/000447364.

34. Shu HC, Hu J, Jiang XB, Deng HQ, Zhang KH. BDNF gene polymorphism and serum level correlate with liver function in patients with hepatitis B-induced cirrhosis. *Int J Clin Exp Pathol*. 2019;12:2368-2380.

35. Stawicka A, Swiderska M, Zbrzeźniak J, et al. Brain-derived neurotrophic factor as a potential diagnostic marker in minimal hepatic encephalopathy. *Clin Exp Hepatol*. 2021;7:117-124. doi:10.5114/ceh.2021.103242.

36. Magen I, Avraham Y, Ackerman Z, Vorobiev L, Mechoulam R, Berry EM. Cannabidiol ameliorates cognitive and motor impairments in mice with bile duct ligation. *J Hepatol*. 2009;51:528-534. doi:10.1016/j.jhep.2009.04.021.

37. Galland F, Negri E, Da Ré C, et al. Hyperammonemia compromises glutamate metabolism and reduces BDNF in the rat hippocampus. *Neurotoxicology*. 2017;62:46-55. doi:10.1016/j.neuro.2017.05.006.

38. Ding S, Xu Z, Yang J, et al. The involvement of the decrease of astrocytic Wnt5a in the cognitive decline in minimal hepatic encephalopathy. *Mol Neu-robiol*. 2017;54:7949-7963. doi:10.1007/s12035-016-0216-5.

39. Dhanda S, Gupta S, Halder A, Sunkaria A, Sandhir R. Systemic inflammation without gliosis mediates cognitive deficits through impaired BDNF expression in bile duct ligation model of hepatic encephalopathy. *Brain Behav Immun*. 2018;70:214-232. doi:10.1016/j.bbi.2018.03.002.

40. Shal B, Khan A, Naveed M, et al. Neuroprotective effect of 25-Methoxyhis-pidol A against CCl<sub>4</sub>-induced behavioral alterations by targeting VEGF/BDNF and caspase-3 in mice. *Life Sci*. 2020;253:117684. doi:10.1016/j.lfs.2020.117684.

41. Görg B, Karababa A, Shafigullina A, Bidmon HJ, Häussinger D. Ammonia-induced senescence in cultured rat astrocytes and in human cerebral cortex in hepatic encephalopathy. *Glia*. 2015;63:37-50. doi:10.1002/glia.22731.

42. Landgraf R. HER2 therapy. HER2 (ERBB2): functional diversity from structurally conserved building blocks. *Breast Cancer Res*. 2007;9:202. doi:10.1186/bcr1633.

43. Tokita Y, Keino H, Matsui F, et al. Regulation of neuregulin expression in the injured rat brain and cultured astrocytes. *JNeurosci*. 2001;21:1257. doi:10.1523/JNEUROSCI.21-04-01257.2001.

44. Jiang R, Chen D, Hou J, et al. Survival and inflammation promotion effect of PTPRO in fulminant hepatitis is associated with NF- $\kappa$ B activation. *JImmu-nol*. 2014;193:5161-5170. doi:10.4049/jimmunol.1303354.

45. Döring P, Calvisi DF, Dombrowski F. Nuclear ErbB2 expression in hepato-cytes in liver disease. *Virchows Arch*. 2021;478:309-318. doi:10.1007/s00428-020-02871-z.

46. Hol EM, Pekny M. Glial fibrillary acidic protein (GFAP) and the astrocyte intermediate filament system in diseases of the central nervous system. *Curr Opin Cell Biol*. 2015;32:121-130. doi:10.1016/j.ceb.2015.02.004.

47. Kretschmar HA, DeArmond SJ, Forno LS. Measurement of GFAP in hepatic encephalopathy by ELISA and transblots. *J Neuropathol Exp Neurol*. 1985;44:459-471. doi:10.1097/00005072-198509000-00002.

48. Balzano T, Forteza J, Molina P, et al. The cerebellum of patients with steato-hepatitis shows lymphocyte infiltration, microglial activation and loss of Purkinje and granular neurons. *Sci Rep*. 2018;8:3004. doi:10.1038/

s41598-018-21399-6.

49. Balzano T, Forteza J, Borreda I, et al. Histological features of cerebellar neuropathology in patients with alcoholic and nonalcoholic steatohepatitis. *J Neuropathol Exp Neurol*. 2018;77:837-845. doi:10.1093/jnen/nly061.

50. Polyak A, Bannykh S, Klein A, Sundaram V. Neurologic imaging in a patient with cirrhosis and altered mental status: to CT or not to CT. *Case Rep Gastro-intest Med*. 2021;2021:5588208. doi:10.1155/2021/5588208.

51. Hiba OE, Elgot A, Ahboucha S, Gamrani H. Differential regional responsiveness of astroglia in mild hepatic encephalopathy: an immunohistochemical approach in bile duct ligated rat. *Acta Histochem*. 2016;118:338-346. doi:10.1016/j.acthis.2016.03.003.

52. Jia W, Liu J, Hu R, et al. Xiaochaihutang improves the cortical astrocyte edema in thioacetamide-induced rat acute hepatic encephalopathy by activating NRF2 pathway. *Front Pharmacol*. 2020;11:382. doi:10.3389/fphar.2020.00382.

53. Chileski GS, García EN, Lértora JW, et al. Hepatic encephalopathy in swine experimentally poisoned with *Senna occidentalis* seeds: effects on astrocytes. *Toxicol*. 2021;201:86-91. doi:10.1016/j.toxicol.2021.08.018.

54. Ferah Okay I, Okay U, Gundogdu OL, et al. Syringic acid protects against thioacetamide-induced hepatic encephalopathy: behavioral, biochemical, and molecular evidence. *Neurosci Lett*. 2022;769:136385. doi:10.1016/j.neulet.2021.136385.

55. Omar EH, Abdelaati EK, Mohamed A, Halima G. P 24 Comparative morphological analysis of astroglia reactivity in the hippocampus of rats with acute and chronic hepatic encephalopathy. *Am J Gastroenterol*. 2019;114:S13.

55. Omar EH, Abdelaati EK, Mohamed A, Halima G. P 24 急性和慢性肝性脑病大鼠海马中星形胶质细胞反应性的比较形态学分析。《美国胃肠病学杂志》。2019 年；114 卷:S13 页。

56. Komatsu A, Iida I, Nasu Y, et al. Ammonia induces amyloidogenesis in astro-

56. Komatsu A, Iida I, Nasu Y 等。氨诱导星形胶质细胞中的淀粉样蛋白生成

cytes by promoting amyloid precursor protein translocation into the endoplasmic reticulum. *J Biol Chem*. 2022;298:101933. doi:10.1016/j.jbc.2022.101933.

57. Back A, Tupper KY, Bai T, et al. Ammonia-induced brain swelling and neurotoxicity in an organotypic slice model. *Neurol Res*. 2011;33:1100-1108.

58. Chastre A, Jiang W, Desjardins P, Butterworth RF. Ammonia and proinflammatory cytokines modify expression of genes coding for astrocytic proteins implicated in brain edema in acute liver failure. *Metab Brain Dis*. 2010;25:17-21. doi:10.1007/s11011-010-9185-y.

59. Salman MM, Kitchen P, Halsey A, et al. Emerging roles for dynamic aquaporin-4 subcellular relocalization in CNS water homeostasis. *Brain*. 2022;145:64-75. doi:10.1093/brain/awab311.

60. Hadjihambi A, Harrison IF, Costas-Rodríguez M, et al. Impaired brain glymphatic flow in experimental hepatic encephalopathy. *J Hepatol*. 2019;70:40-49. doi:10.1016/j.jhep.2018.08.021.

61. Thumburu KK, Dhiman RK, Vasishta RK, et al. Expression of astrocytic genes coding for proteins implicated in neural excitation and brain edema is altered after acute liver failure. *J Neurochem*. 2014;128:617-627. doi:10.1111/jnc.12511.

62. Shulyatnikova T, Tumanskiy V. Immunohistochemical study of the brain aquaporin-4 in the rat acute liver failure model. *Art Med*. 2022;21:103-108.

63. Abo El, Gheit RE, Atef MM, Badawi GA, Elwan WM, Alshenawy HA, Emam MN. Role of serine protease inhibitor, ulinastatin, in rat model of hepatic encephalopathy: aquaporin 4 molecular targeting and therapeutic implication. *J Physiol Biochem*. 2020;76:573-586. doi:10.1007/s13105-020-00762-0.

64. Dhanda S, Sandhir R. Blood-brain barrier permeability is exacerbated in experimental model of hepatic encephalopathy via MMP-9 activation and downregulation of tight junction proteins. *Mol Neurobiol.* 2018;55:3642-3659. doi:10.1007/s12035-017-0521-7.
65. Rama Rao KV, Verkman AS, Curtis KM, Norenberg MD. Aquaporin-4 deletion in mice reduces encephalopathy and brain edema in experimental acute liver failure. *Neurobiol Dis.* 2014;63:222-228. doi:10.1016/j.nbd.2013.11.018.
66. Wright G, Soper R, Brooks HF, et al. Role of aquaporin-4 in the development of brain oedema in liver failure. *J Hepatol.* 2010;53:91-97. doi:10.1016/j.jhep.2010.02.020.
67. Rama Rao KV, Jayakumar AR, Tong X, Curtis KM, Norenberg MD. Brain aquaporin-4 in experimental acute liver failure. *J Neuropathol Exp Neurol.* 2010;69:869-879. doi:10.1097/NEN.0b013e3181ebe581.
68. Eefsen M, Jelles P, Schmidt LE, Vainer B, Bisgaard HC, Larsen FS. Brain expression of the water channels Aquaporin-1 and -4 in mice with acute liver injury, hyperammonemia and brain edema. *Metab Brain Dis.* 2010;25:315-323. doi:10.1007/s11011-010-9213-y.
69. Bodega G, Suárez I, López-Fernández LA, et al. Ammonia induces aquaporin-4 rearrangement in the plasma membrane of cultured astrocytes. *Neurochem Int.* 2012;61:1314-1324. doi:10.1016/j.neuint.2012.09.008.
70. Rama Rao KV, Chen M, Simard JM, Norenberg MD. Increased aquaporin-4 expression in ammonia-treated cultured astrocytes. *Neuroreport.* 2003;14:2379-2382. doi:10.1097/00001756-200312190-00018.
71. Zhou Y, Danbolt N. GABA and glutamate transporters in brain. *Front Endocrinol.* 2013;4:165. doi:10.3389/fendo.2013.00165.
72. Wen FF, Xu Z, Liu LP, Yang JJ, Ding SD. [Effect of dopamine on intracerebral glutamate uptake ability in rats with minimal hepatic encephalopathy and the pathogenesis of minimal hepatic encephalopathy]. *Zhonghua Gan Zang Bing Za Zhi.* 2018;26:48-53. doi:10.3760/cma.j.issn.1007-3418.2018.01.011.
73. Suárez I, Bodega G, Fernández B. Modulation of glutamate transporters (GLAST, GLT-1 and EAAC1) in the rat cerebellum following portocaval anastomosis. *Brain Res.* 2000;859:293-302. doi:10.1016/s0006-8993(00)01993-4.
74. Chan H, Butterworth RF. Evidence for an astrocytic glutamate transporter deficit in hepatic encephalopathy. *Neurochem Res.* 1999;24:1397-1401. doi:10.1023/a:1022532623281.
75. Butterworth RF. Glutamate transporters in hyperammonemia. *Neurochem Int.* 2002;41:81-85. doi:10.1016/s0197-0186(02)00027-x.
76. Jiménez-Torres C, El-Kehdy H, Hernández-Kelly LC, et al. Acute liver toxicity modifies protein expression of glutamate transporters in liver and cerebellar tissue. *Front Neurosci.* 2021;14:613225. doi:10.3389/fnins.2020.613225.
77. Mitchell RW, On NH, Del Bigio MR, Miller DW, Hatch GM. Fatty acid transport protein expression in human brain and potential role in fatty acid transport across human brain microvessel endothelial cells. *J Neurochem.* 2011;117:735-746.
78. Ouellet M, Emond V, Chen CT, et al. Diffusion of docosahexaenoic and eicosapentaenoic acids through the blood-brain barrier: an in situ cerebral perfusion study. *Neurochem Int.* 2009;55:476-482.
79. Lee JA, Hall B, Allsop J, Alqarni R, Allen SP. Lipid metabolism in astrocytic structure and function. *Semin Cell Dev Biol.* 2021;112:123-136.
80. Andersen JV, Westi EW, Jakobsen E, Urruticoechea N, Borges K, Aldana BI. Astrocyte metabolism of the medium-chain fatty acids octanoic acid and deca-noic acid promotes GABA synthesis in neurons via elevated glutamine supply. *Mol Brain.* 2021;14:132. doi:10.1186/s13041-021-00842-2.
81. Eraso-Pichot A, Brasó-Vives M, Golbano A, et al. GSEA of mouse and human mitochondriomes reveals fatty acid oxidation in astrocytes. *Glia.* 2019;66:1724-1735.
82. Morita M, Shinbo S, Asahi A, Imanaka T. Very long chain fatty acid  $\beta$  - oxidation in astrocytes: contribution of the ABCD1-dependent and -independent pathways. *Biol Pharm Bull.* 2012;35:1972-1979. doi:10.1248/bpb.12-00411.

83. Fecher C, Trovò L, Müller SA, et al. Cell-type-specific profiling of brain mitochondria reveals functional and molecular diversity. *Nat Neurosci.* 2019;22:1731-1742. doi:10.1038/s41593-019-0479-z.
84. Houten SM, Wanders RJ. A general introduction to the biochemistry of mitochondrial fatty acid  $\beta$  -oxidation. *J Inher Metab Dis.* 2010;33:469-477.
85. Jernberg JN, Bowman CE, Wolfgang MJ, Scafidi S. Developmental regulation and localization of carnitine palmitoyltransferases (CPT s) in rat brain. *J Neurochem.* 2017;142:407-419.
86. Boer LA, Panatto JP, Fagundes DA, et al. Inhibition of mitochondrial respiratory chain in the brain of rats after hepatic failure induced by carbon tetrachloride is reversed by antioxidants. *Brain Res Bull.* 2009;80:75-78.
87. Astore D, Boicelli CA. Hyperammonemia and chronic hepatic encephalopathy: an in vivo PMRS study of the rat brain. *MAGMA.* 2000;10:160-166. doi:10.1007/BF02590641.
88. Drews L, Zimmermann M, Poss RE, et al. Ammonia inhibits energy metabolism in astrocytes in a rapid and GDH2-dependent manner. *bioRxiv* 683763, 2019. doi:10.1101/683763.
89. Haghighat N, McCandless DW. Effect of ammonium chloride on energy metabolism of astrocytes and C6-glioma cells in vitro. *Metab Brain Dis.* 1997;12:287-298. doi:10.1007/bf02674673.
90. Bai G, Rama Rao KV, Murthy CR, et al. Ammonia induces the mitochondrial permeability transition in primary cultures of rat astrocytes. *J Neurosci Res.* 2001;66:981-991.
91. Chan H, Hazell AS, Desjardins P, Butterworth RF. Effects of ammonia on glutamate transporter (GLAST) protein and mRNA in cultured rat cortical astrocytes. *Neurochem Int.* 2000;37:243-248.
92. Palomero-Gallagher N, Zilles K. Neurotransmitter receptor alterations in hepatic encephalopathy: a review. *Arch Biochem Biophys.* 2013;536:109-121. doi:10.1016/j.abb.2013.02.010.
93. Michalak A, Chatauret N, Butterworth RF. Evidence for a serotonin transporter deficit in experimental acute liver failure. *Neurochem Int.* 2001;38:163- 168. doi:10.1016/s0197-0186(00)00062-0.
94. Rao VLR, Butterworth RF. Alterations of [3H]8-OH-DPAT and [3H]ketan-serin binding sites in autopsied brain tissue from cirrhotic patients with hepatic encephalopathy. *Neurosci Lett.* 1994;182:69-72. doi:10.1016/0304-3940(94)90208-9.
95. Lozeva V, Montgomery JA, Tuomisto L, et al. Increased brain serotonin turnover correlates with the degree of shunting and hyperammonemia in rats following variable portal vein stenosis. *J Hepatol.* 2004;40:742-748. doi:10.1016/j.jhep.2004.01.003.
96. Quillet A, Saad C, Ferry G, et al. Improving bioinformatics prediction of microRNA targets by ranks aggregation. *Front Genet.* 2020;10:1330. doi:10.3389/fgene.2019.01330.
97. Manzhali E, Virchenko O, Falalyeyeva T, et al. Hepatic encephalopathy aggravated by systemic inflammation. *Dig Dis.* 2019;37:509-517. doi:10.1159/000500717.
98. Cauli O, Rodrigo R, Piedrafita B, Boix J, Felipe V. Inflammation and hepatic encephalopathy: ibuprofen restores learning ability in rats with portacaval shunts. *Hepatology.* 2007;46:514-519. doi:10.1002/hep.21734.
99. Patidar KR, Bajaj JS. Antibiotics for the treatment of hepatic encephalopathy. *Metab Brain Dis.* 2013;28:307-312. doi:10.1007/s11011-013-9383-5.
100. Tarao K, Ikeda T, Hayashi K, et al. Successful use of vancomycin hydrochloride in the treatment of lactulose resistant chronic hepatic encephalopathy. *Gut.* 1990;31:702. doi:10.1136/gut.31.6.702.
101. Forbes A, Murray-Lyon I. Vancomycin in resistant hepatic encephalopathy. *Gut.* 1990;31:1424-1424. doi:10.1136/gut.31.12.1424-b.
102. Kuzuya T, Takeda K, Utsunomiya S, et al. [A case of intractable hepatic encephalopathy successfully treated by oral administration of vancomycin hydrochloride, with subsequent improvement of hepatic function reserve enabling transcatheter arterial chemoembolization against hepatocellular carcinoma]. *Gan to Kagaku Ryoho.* 2011;38:995-997.

103. Walayat S, Shoaib H, Asghar M, Kim M, Dhillon S. Role of N-acetylcysteine in non-acetaminophen-related acute liver failure: an updated meta-analysis and systematic review. *Ann Gastroenterol.* 2021;34:235-240. doi:10.20524/aog.2021.0571.
104. Mohammadi H, Sayad A, Mohammadi M, Niknahad H, Heidari R. N-acetyl cysteine treatment preserves mitochondrial indices of functionality in the brain of hyperammonemic mice. *Clin Exp Hepatol.* 2020;6:106-115. doi:10.5114/ceh.2020.95814.
105. López A, Chavarría R, Oviedo G. Therapeutic dilemma: alcohol withdrawal syndrome and concurrent hepatic encephalopathy. A case report. *Rev Colomb Psiquiatr (Engl Ed).* 2021;50:52-56. doi:10.1016/j.rcpeng.2019.10.002.
106. Chaplin AC, Curley MA, Wanless IR. Re: recent case report of clozapine-induced acute hepatic failure. *Can J Gastroenterol.* 2010;24:739-740; author reply 741. doi:10.1155/2010/535026.
107. Shah J, Muir J, Furfaro D, Beitler JR, Dzierba AL. Use of N-acetylcysteine for clozapine-induced acute liver injury: a case report and literature review [published online ahead of print July 20, 2021]. *J Pharm Pract.* doi:10.117708971900211034007.
108. Yen FS, Yang YC, Hwu CM, et al. Liver-related long-term outcomes of thia-zolidinedione use in persons with type 2 diabetes. *Liver Int.* 2020;40:1089- 1097. doi:10.1111/liv.14385.
109. Bekpinar S, Vardagli D, Unlucerci Y, Can A, Uysal M, Gurdol F. Effect of rosiglitazone on asymmetric dimethylarginine metabolism in thioacetamide-induced acute liver injury. *Pathophysiology.* 2015;22:153-157. doi:10.1016/j.pathophys.2015.06.003.
110. Abdel-Salam OM, Shaffie NM, Mohammed NA, et al. The 5-HT1A agonist buspirone decreases liver oxidative stress and exerts protective effect against CCl4-toxicity. *J Exp Clin Toxicol.* 2017;1:13-26.